PSAS'2016

International Conference on
Precision Physics of Simple Atomic Systems

Higher Order Corrections to Positronium Energies

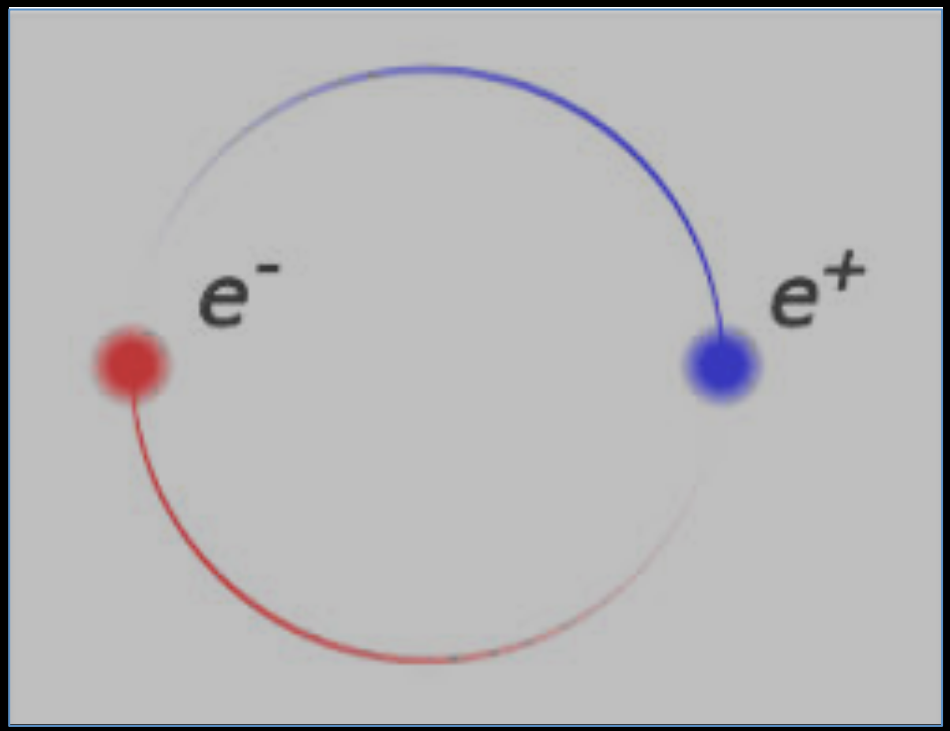

Greg Adkins
Franklin & Marshall College

and collaborators:

Dick Fell
(Brandeis University)

Minji Kim Christian Parsons
Matt Salinger Ruihan Wang
Lam Tran Tomass Brazovskis
Xuan Zhang Dimitrios Tsaras
(Franklin & Marshall College)

Higher Order Corrections to Positronium Energies

Motivation
Experimental Situation
Theoretical Methods
Recent Progress and Present Status

Acknowledgments
NSF PHY-1404268
Franklin & Marshall College

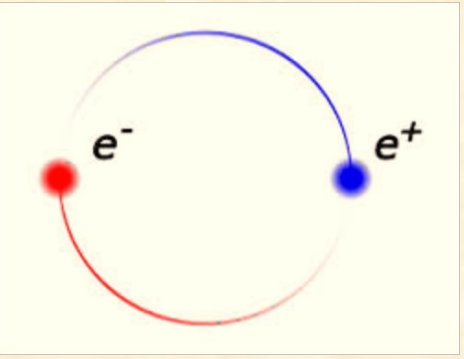

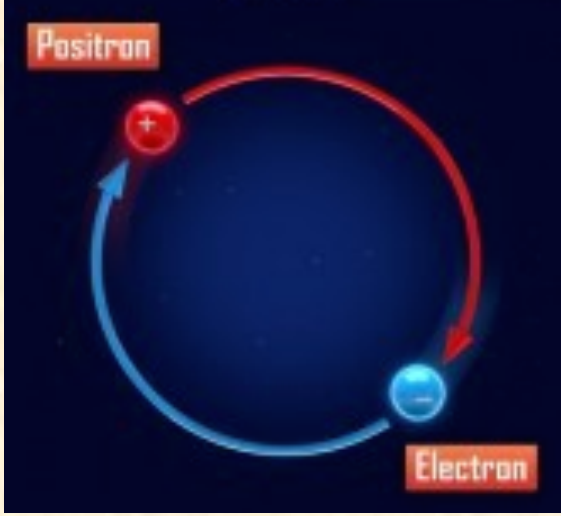

Why Study Positronium?

Positronium is intrinsically interesting. It is the simplest bound system. It's constituents are structureless pointlike particles. Many fundamental aspects of quantum field theory enter into its description. It differs from other exotic atoms in having large recoil effects, little sensitivity to hadronic physics, and is subject to real and virtual annihilation.

Positronium is accessible both to high precision experiments and to detailed calculations, so its study allows for a stringent test of the theory of bound states in QED (quantum electrodynamics) and quantum field theory generally.

Positronium is ideal for tests of fundamental symmetries and is useful in searches for "new physics".

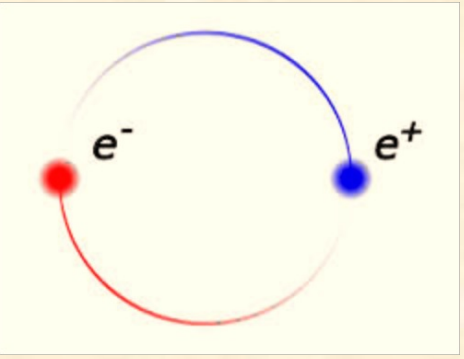

Positronium Spectrum

The n=1 and n=2 levels of positronium are shown. (Transition energies are in units of MHz.)

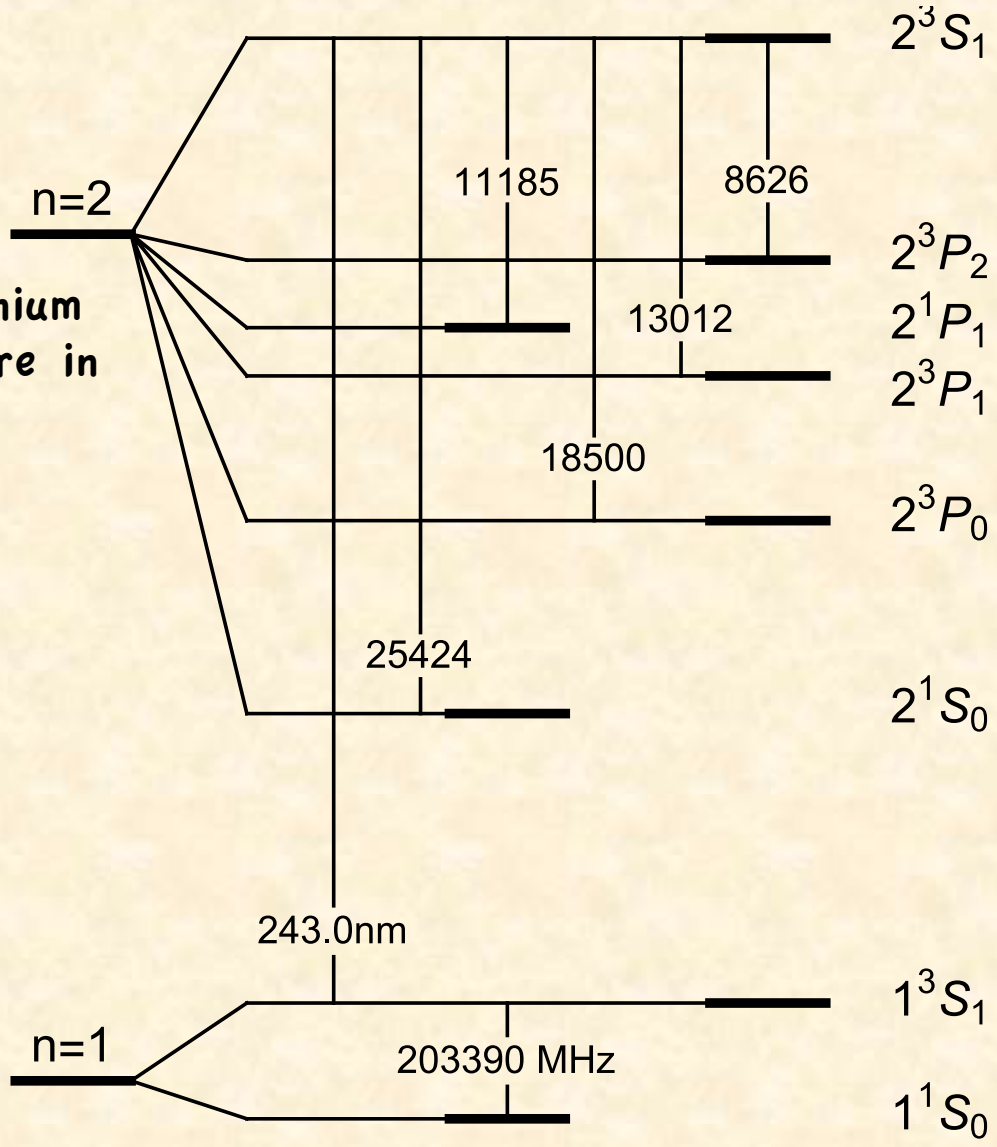

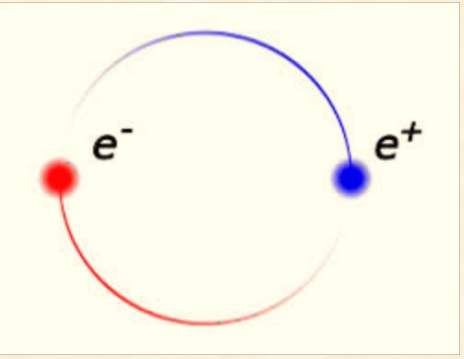

Positronium Spectrum

The n=1 and n=2 levels of positronium are shown. Transitions of experimental interest are the

(1) n=1 hyperfine splitting $(1^3S_1 - 1^1S_0)$

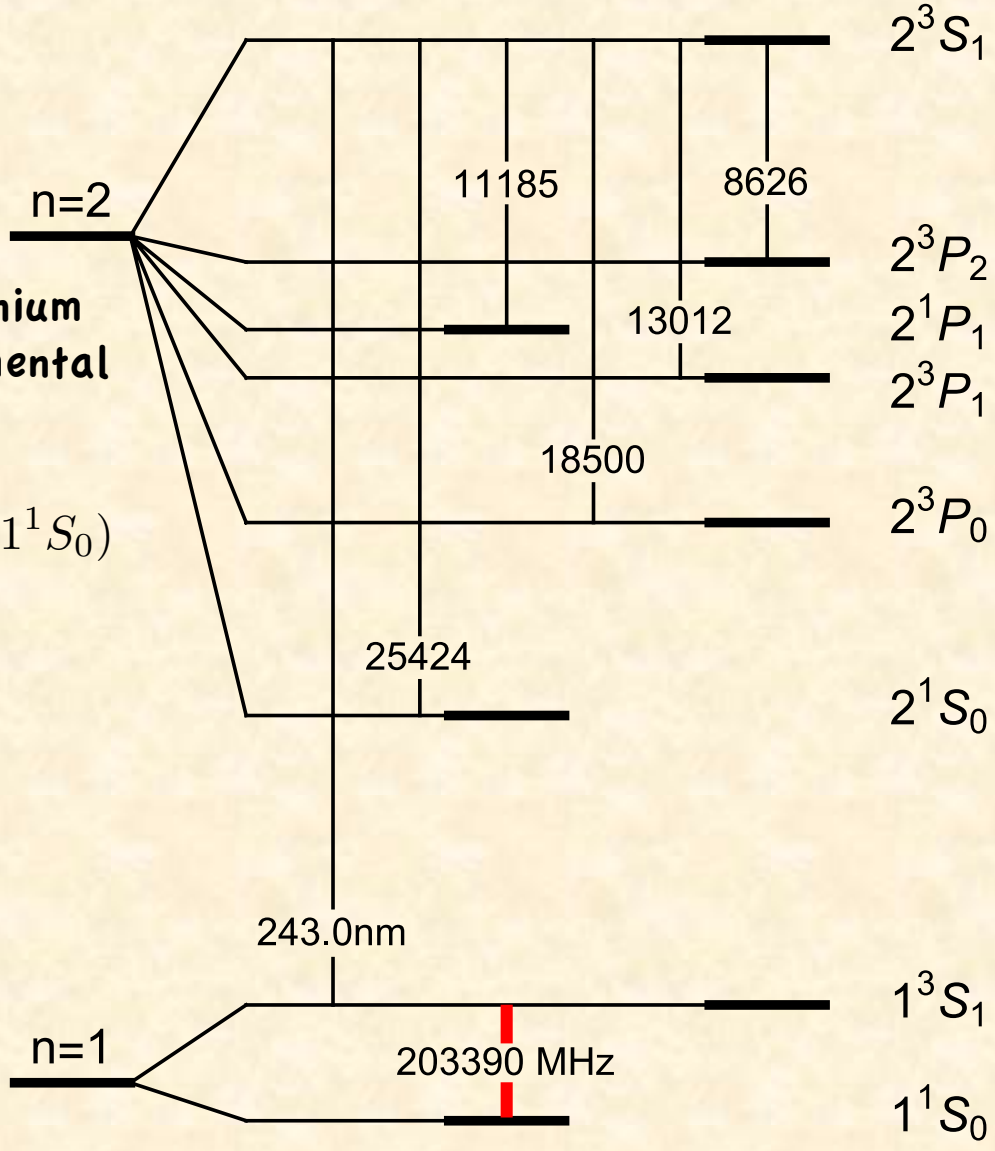

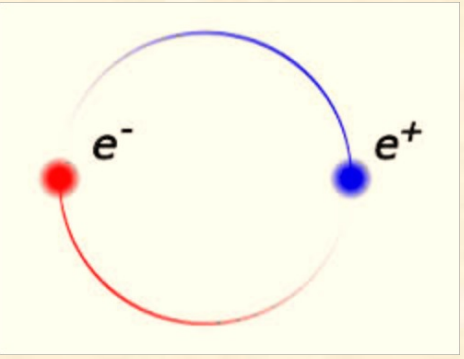

Positronium Spectrum

The n=1 and n=2 levels of positronium are shown. Transitions of experimental interest are the

(1) n=1 hyperfine splitting $(1^3S_1 - 1^1S_0)$

(2) n=2 fine structure $(2^3S_1 - 2P)$

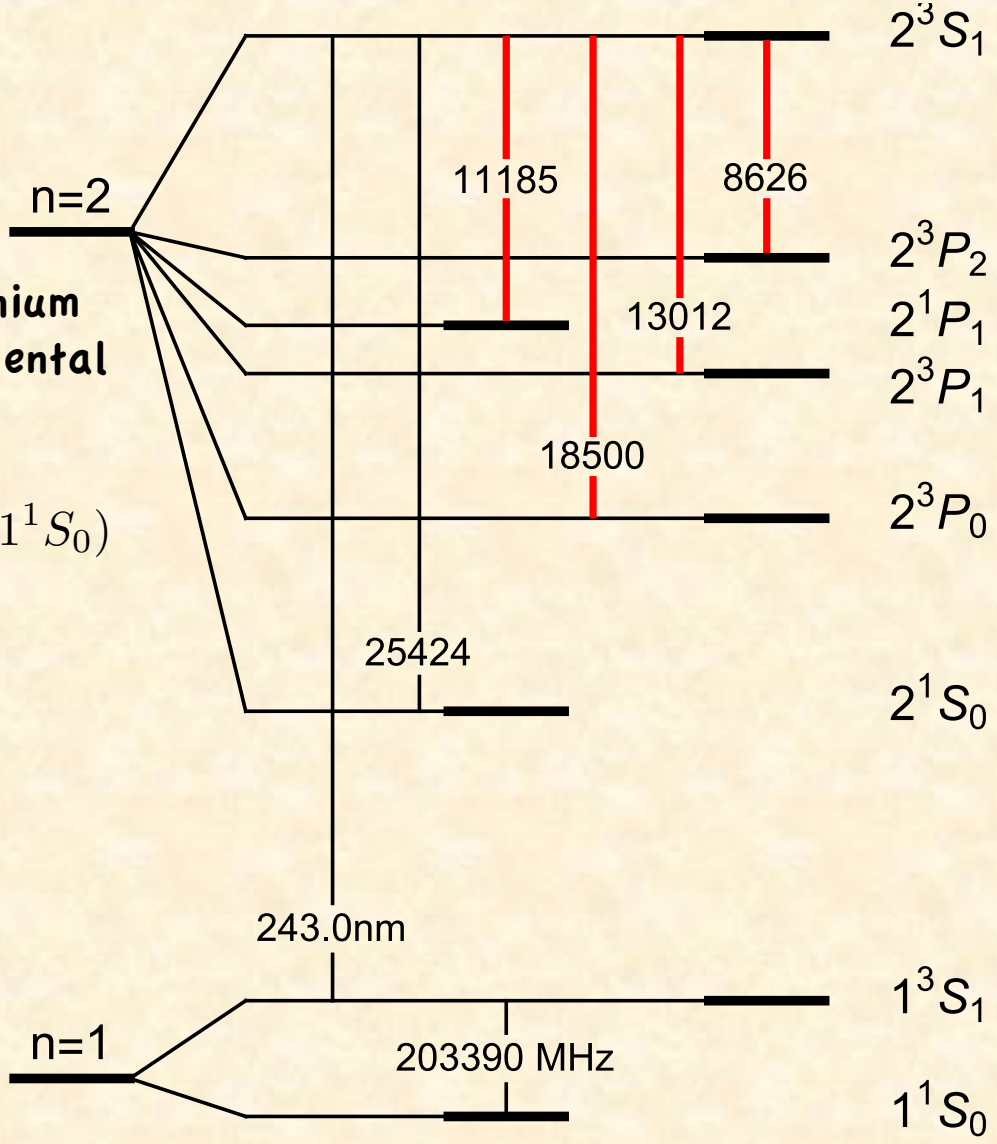

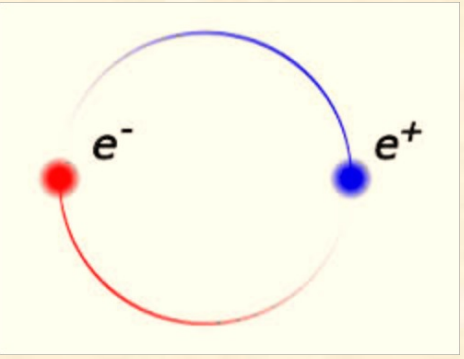

Positronium Spectrum

The n=1 and n=2 levels of positronium are shown. Transitions of experimental interest are the

(1) n=1 hyperfine splitting $(1^3S_1 - 1^1S_0)$

(2) n=2 fine structure $(2^3S_1 - 2P)$

(3) 2S-1S transition $(2^3S_1 - 1^3S_1)$

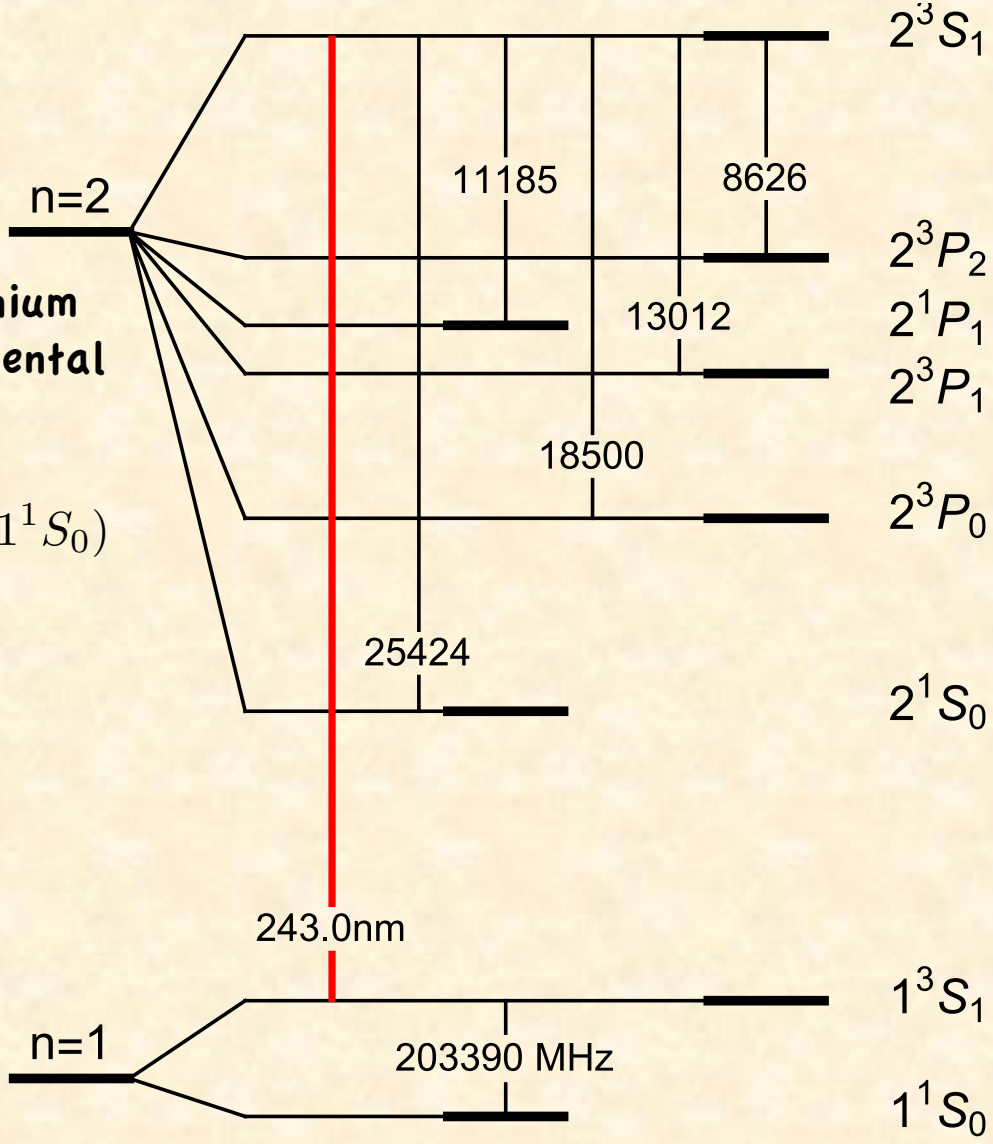

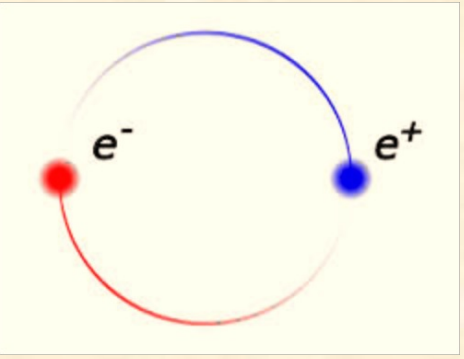

Positronium Spectrum

The n=1 and n=2 levels of positronium are shown. Transitions of experimental interest are the

(1) n=1 hyperfine splitting $(1^3S_1 - 1^1S_0)$

(2) n=2 fine structure $(2^3S_1 - 2P)$

(3) 2S-1S transition $(2^3S_1 - 1^3S_1)$

All of the measurements have uncertainties on the order of 1MHz

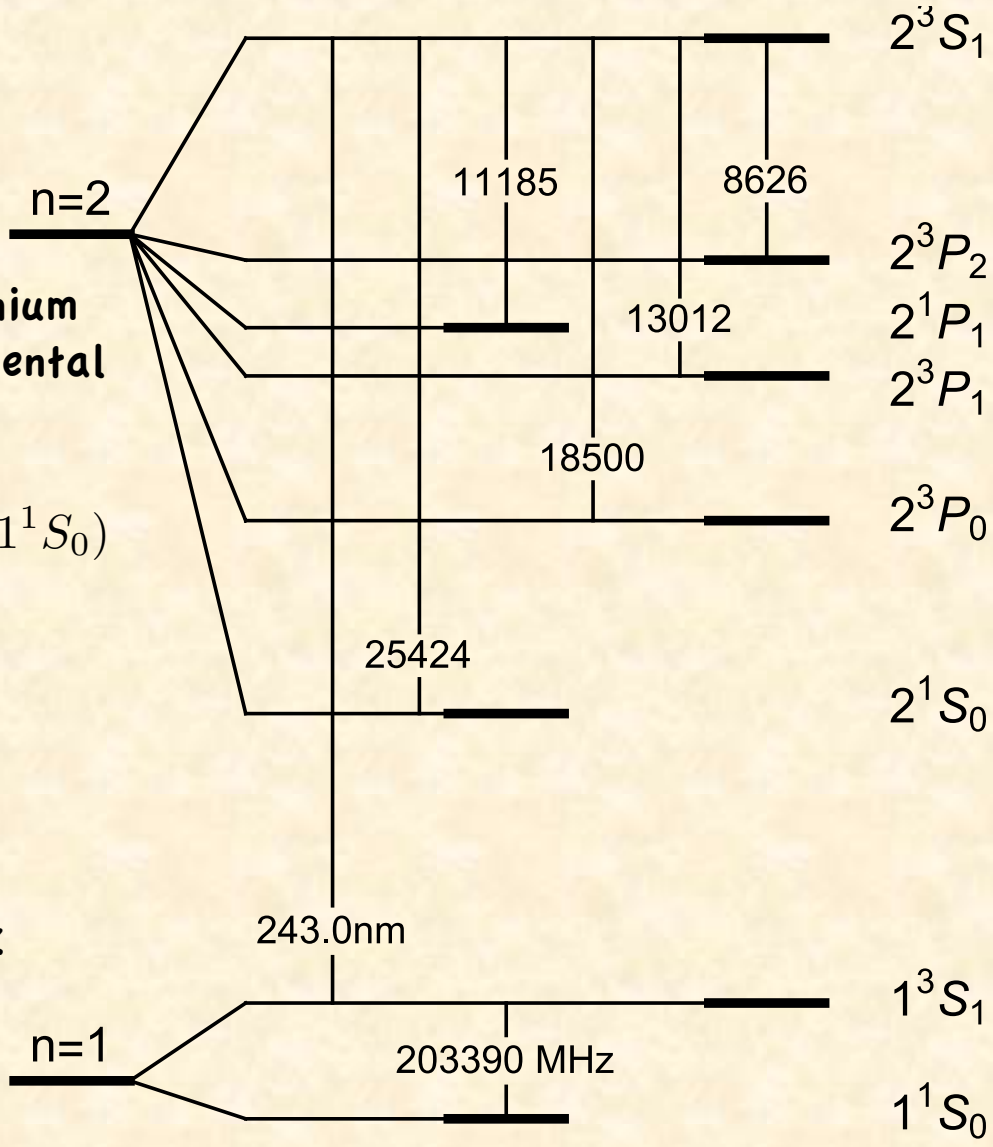

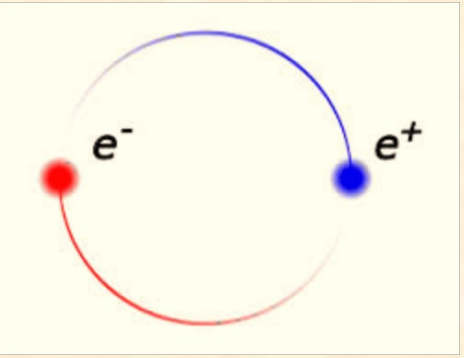

Hyperfine Structure

This table shows the two main periods of experimental work on the positronium hyperfine interval: the 1950s and the 1970s. The present era promises to be a third such exciting period of progress.

TABLE I: Experimental Results for the Positronium Hyperfine Interval

Year	Frequency Shift	Precision	Experimenters
1951	227(34) GHz	15%	Deutsch and Dulit
1952	203.2(3) GHz	1477 ppm	Deutsch and Brown
1954	203350(50) MHz	246 ppm	Weinstein, Deutsch, and Brown
1955	203380(40) MHz	197 ppm	Weinstein, Deutsch, and Brown
1957	203330(40) MHz	197 ppm	Hughes, Marder, and Wu
1970	203403(12) MHz	59 ppm	Theriot, Beers, Hughes, and Zioch
1972	203396(5) MHz	25 ppm	Carlson, Hughes, Lewis, and Lindgren
1975	203387.0(1.6) MHz	8 ppm	Mills and Bearman
1977	203384(4) MHz	20 ppm	Carlson, Hughes, and Lindgren
1977	203384.9(1.2) MHz	6 ppm	Egan, Hughes, and Yam
1983	203387.5(1.6) MHz	8 ppm	Mills ("Line-shape effects")
1984	203389.10(74) MHz	3.6 ppm	Ritter, Egan, Hughes, and Woodle
2014	203394.2 $(1.6)_{stat}(1.3)_{sys}$ MHz	10 ppm	Ishida, Namba, Asai, Kobayashi, Saito, Yoshida, Tanaka, and Yamamoto

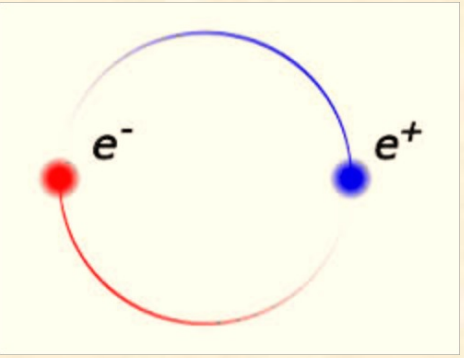

Hyperfine Structure

This table shows the two main periods of experimental work on the positronium hyperfine interval: the 1950s and the 1970s. The present era promises to be a third such exciting period of progress.

TABLE I: Experimental Results for the Positronium Hyperfine Interval

Year	Frequency Shift	Precision	Experimenters
1951	227(34) GHz	15%	Deutsch and Dulit
1952	203.2(3) GHz	1477 ppm	Deutsch and Brown
1954	203350(50) MHz	246 ppm	Weinstein, Deutsch, and Brown
1955	203380(40) MHz	197 ppm	Weinstein, Deutsch, and Brown
1957	203330(40) MHz	197 ppm	Hughes, Marder, and Wu
1970	203403(12) MHz	59 ppm	Theriot, Beers, Hughes, and Zioch
1972	203396(5) MHz	25 ppm	Carlson, Hughes, Lewis, and Lindgren
1975	203387.0(1.6) MHz	8 ppm	Mills and Bearman
1977	203384(4) MHz	20 ppm	Carlson, Hughes, and Lindgren
1977	203384.9(1.2) MHz	6 ppm	Egan, Hughes, and Yam
1983	203387.5(1.6) MHz	8 ppm	Mills ("Line-shape effects")
1984	203389.10(74) MHz	3.6 ppm	Ritter, Egan, Hughes, and Woodle
2014	203394.2 $(1.6)_{stat}(1.3)_{sys}$ MHz	10 ppm	Ishida, Namba, Asai, Kobayashi, Saito, Yoshida, Tanaka, and Yamamoto

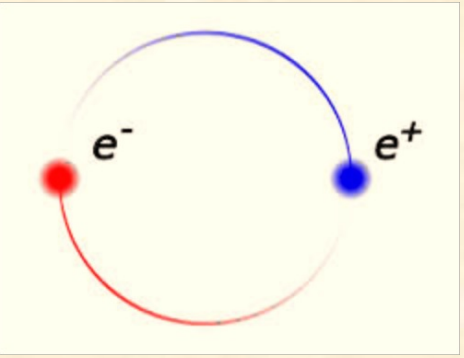

Hyperfine Structure

This table shows the two main periods of experimental work on the positronium hyperfine interval: the 1950s and the 1970s. The present era promises to be a third such exciting period of progress.

TABLE I: Experimental Results for the Positronium Hyperfine Interval

Year	Frequency Shift	Precision	Experimenters
1951	227(34) GHz	15%	Deutsch and Dulit
1952	203.2(3) GHz	1477 ppm	Deutsch and Brown
1954	203350(50) MHz	246 ppm	Weinstein, Deutsch, and Brown
1955	203380(40) MHz	197 ppm	Weinstein, Deutsch, and Brown
1957	203330(40) MHz	197 ppm	Hughes, Marder, and Wu
1970	203403(12) MHz	59 ppm	Theriot, Beers, Hughes, and Zioch
1972	203396(5) MHz	25 ppm	Carlson, Hughes, Lewis, and Lindgren
1975	203387.0(1.6) MHz	8 ppm	Mills and Bearman
1977	203384(4) MHz	20 ppm	Carlson, Hughes, and Lindgren
1977	203384.9(1.2) MHz	6 ppm	Egan, Hughes, and Yam
1983	203387.5(1.6) MHz	8 ppm	Mills ("Line-shape effects")
1984	203389.10(74) MHz	3.6 ppm	Ritter, Egan, Hughes, and Woodle
2014	203394.2 $(1.6)_{stat}(1.3)_{sys}$ MHz	10 ppm	Ishida, Namba, Asai, Kobayashi, Saito, Yoshida, Tanaka, and Yamamoto

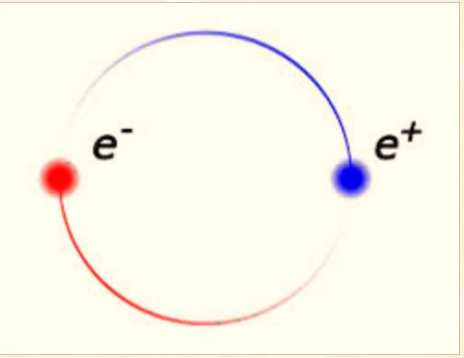

Hyperfine Structure

This table shows the two main periods of experimental work on the positronium hyperfine interval: the 1950s and the 1970s. The present era promises to be a third such exciting period of progress.

TABLE I: Experimental Results for the Positronium Hyperfine Interval

Year	Frequency Shift	Precision	Experimenters
1951	227(34) GHz	15%	Deutsch and Dulit
1952	203.2(3) GHz	1477 ppm	Deutsch and Brown
1954	203350(50) MHz	246 ppm	Weinstein, Deutsch, and Brown
1955	203380(40) MHz	197 ppm	Weinstein, Deutsch, and Brown
1957	203330(40) MHz	197 ppm	Hughes, Marder, and Wu
1970	203403(12) MHz	59 ppm	Theriot, Beers, Hughes, and Zioch
1972	203396(5) MHz	25 ppm	Carlson, Hughes, Lewis, and Lindgren
1975	203387.0(1.6) MHz	8 ppm	Mills and Bearman
1977	203384(4) MHz	20 ppm	Carlson, Hughes, and Lindgren
1977	203384.9(1.2) MHz	6 ppm	Egan, Hughes, and Yam
1983	203387.5(1.6) MHz	8 ppm	Mills ("Line-shape effects")
1984	203389.10(74) MHz	3.6 ppm	Ritter, Egan, Hughes, and Woodle
2014	203394.2 $(1.6)_{stat}(1.3)_{sys}$ MHz	10 ppm	Ishida, Namba, Asai, Kobayashi, Saito, Yoshida, Tanaka, and Yamamoto

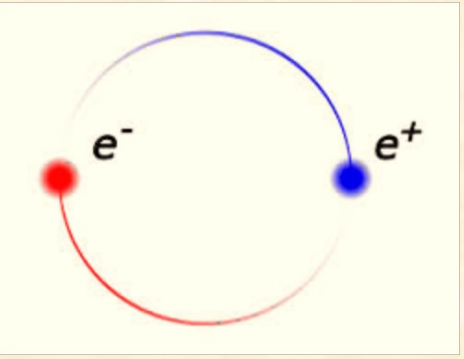

Hyperfine Structure

The experimental situation for the hyperfine structure is somewhat problematic. The experimental results shown are the result of many years of work of increasing precision, completed in 1984.

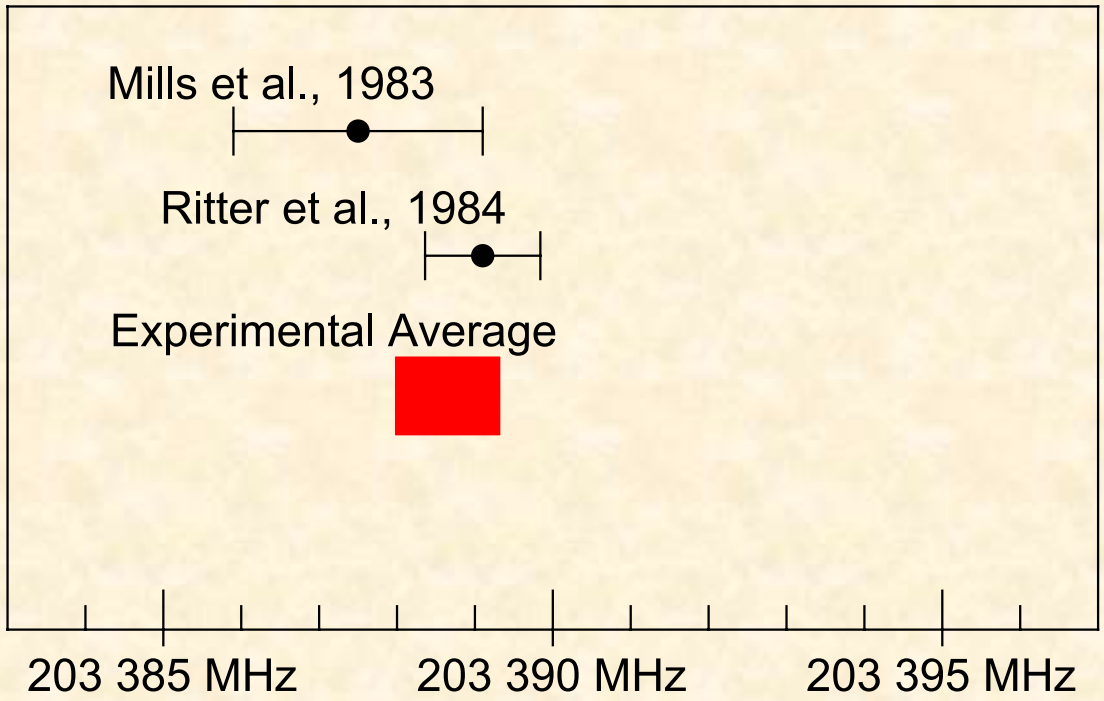

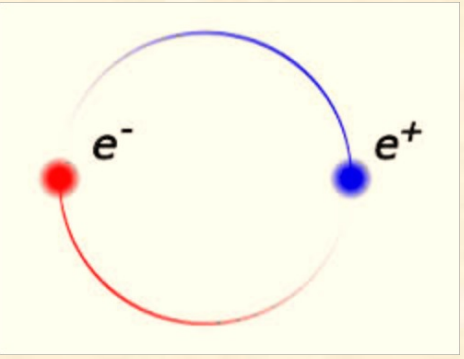

Hyperfine Structure

The experimental situation for the hyperfine structure is somewhat problematic. The experimental results shown are the result of many years of work of increasing precision, completed in 1984.

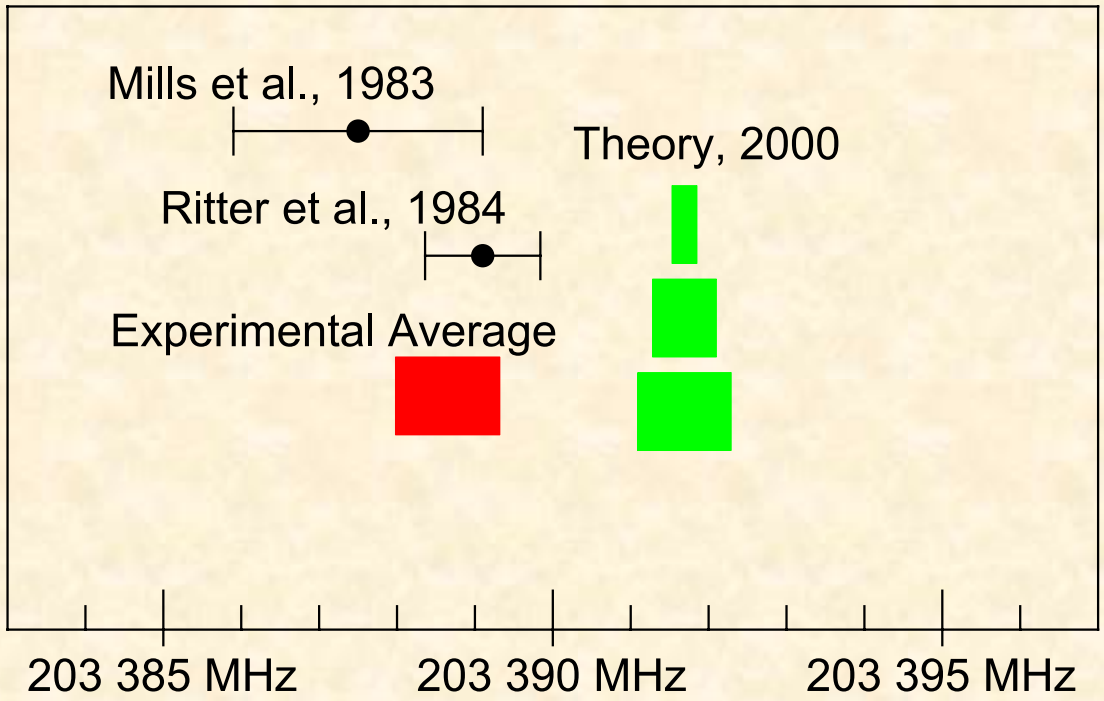

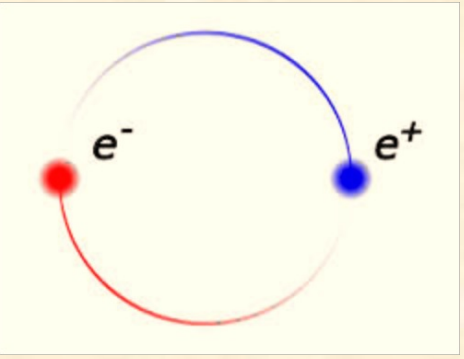

Hyperfine Structure
Experiment vs. Theory

A recent result by the Tokyo group throws perhaps a new light on the situation. Additional experimental work with the promise of new ppm measurements is ongoing.

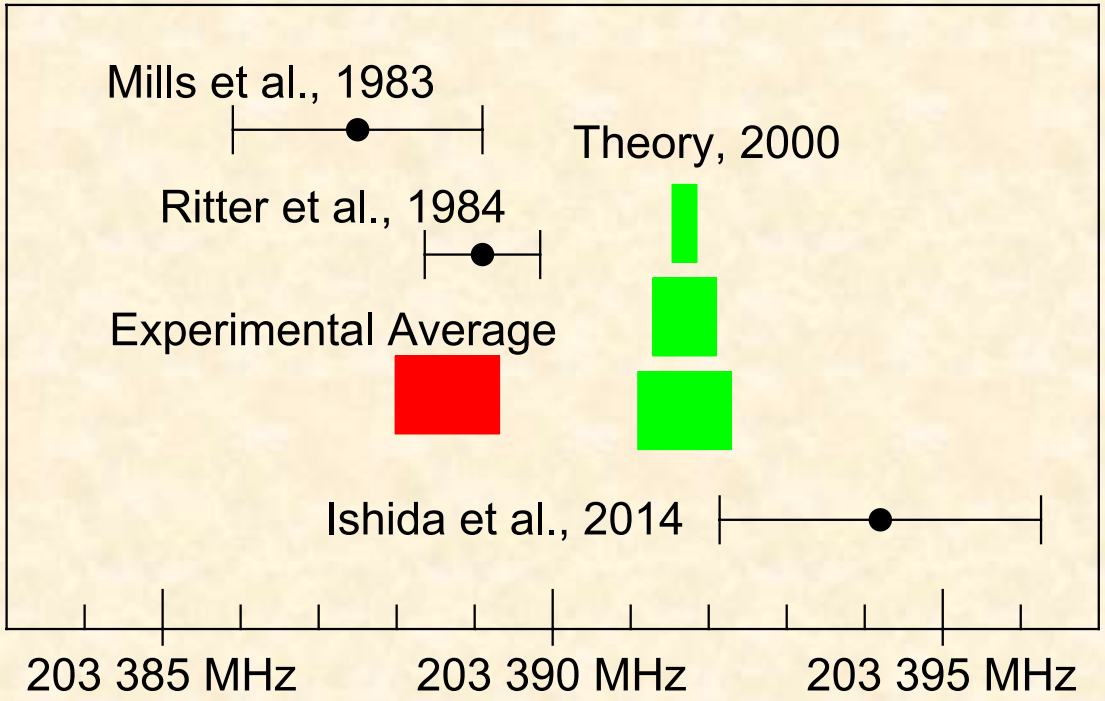

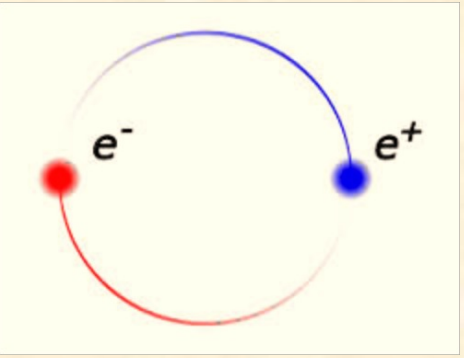

Measured Transitions

Transition	Common Name	Natural Linewidth	Expt. Uncert.
$1^3S_1 - 1^1S_0$	n=1 hyperfine	≈1300MHz	≈1MHz
$2^3S_1 - 2P$	n=2 fine structure	≈50MHz	≈2MHz
$2^3S_1 - 1^3S_1$	2S-1S	≈1.3MHz	≈3MHz

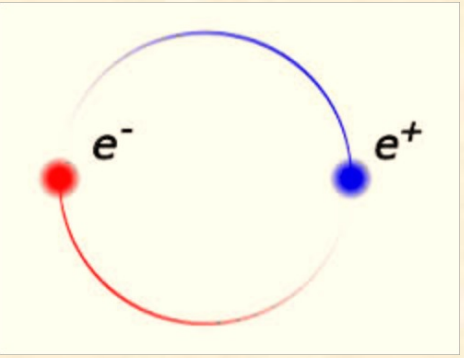

Measured Transitions

Transition	Common Name	Natural Linewidth	Expt. Uncert.
$1^3S_1 - 1^1S_0$	n=1 hyperfine	≈1300MHz	≈1MHz
$2^3S_1 - 2P$	n=2 fine structure	≈50MHz	≈2MHz
$2^3S_1 - 1^3S_1$	2S-1S	≈1.3MHz	≈3MHz

2S-1S ΔE=1233607216.4(3.2) MHz (2.6ppb)
seems to have the greatest potential for improvement.

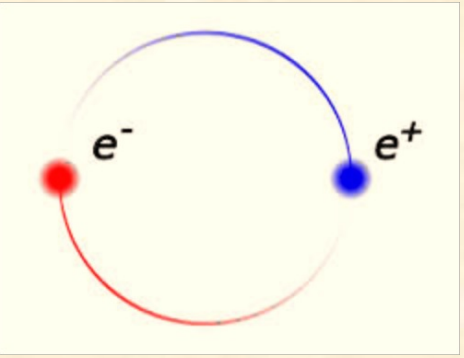

Hyperfine Structure
Status as of 2000

The theoretical formula for the hyperfine splitting can be written as

$$\Delta E = m\alpha^4\left\{C_0 + C_1\frac{\alpha}{\pi} + C_{21}\alpha^2\ln\left(\frac{1}{\alpha}\right) + C_{20}\left(\frac{\alpha}{\pi}\right)^2 + C_{32}\frac{\alpha^3}{\pi}\ln^2\left(\frac{1}{\alpha}\right) + C_{31}\frac{\alpha^3}{\pi}\ln\left(\frac{1}{\alpha}\right) + C_{30}\left(\frac{\alpha}{\pi}\right)^3 + \cdots\right\}$$

where all terms through the order α^3 logarithmic corrections were known by 2000. The numerical value was found to be

$$\Delta E = 203389.69 MHz$$

with an uncertainty variously estimated to be 0.16MHz to 0.6MHz. This uncertainty is comparable to the experimental uncertainty, and should be reduced by computing the α^3 non-log contributions.

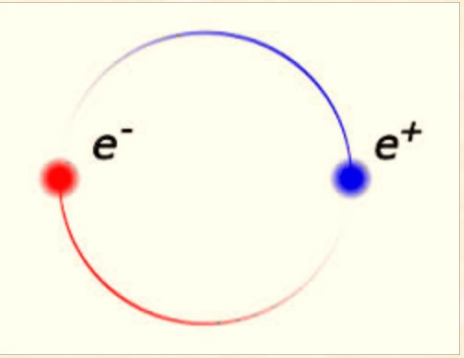

Hyperfine Structure
Status as of 2000

The natural order of ("hard") three-loop corrections is

$$\frac{m\alpha^7}{\pi^3} \approx 0.00439 MHz$$

None of the C's is particularly big—the largest being C_{20}=-3.877. In order to describe a correction that amounts to 0.6MHz, C_{30} would have to be quite large—about $14\pi^2 \approx 138$. Such large contributions to C have indeed been found.

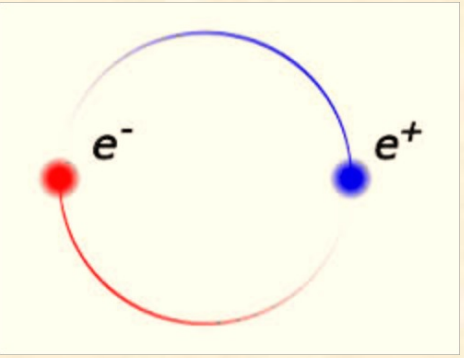

Energy Level Contributions at Order $m\alpha^7$

The present challenge is to complete the calculation of all corrections of order $m\alpha^7$. We use an approach to this problem based on Non-Relativistic QED: NRQED. NRQED is an effective quantum field theory constructed to match the full QED at low energies (much smaller than the electron rest energy). The fundamental degrees of freedom of NRQED are the electron field $\psi(x)$, (which is a 2-component Pauli spinor field), a similar but independent positron field, and the usual photon field.

The NRQED Lagrangian contains coefficients that are determined by "matching": making sure that predictions for low-energy effects—such as low energy electron-positron scattering—that can be calculated using NRQED, agree with predictions for the same processes obtained using QED.

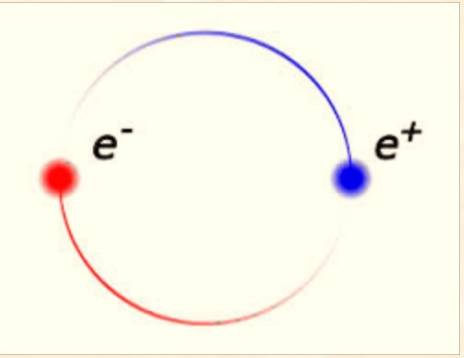

Lagrangian of NRQED

$$\mathcal{L} = \psi^\dagger \Big\{ iD_t + \frac{\vec{D}^{\,2}}{2m} + \frac{\vec{D}^{\,4}}{8m^3} + c_F \frac{q}{2m} \vec{\sigma} \cdot \vec{B} + c_D \frac{q}{2m^2} [\vec{\nabla} \cdot \vec{E}]$$
$$+ c_S \frac{iq}{8m^2} \vec{\sigma} \cdot \Big(\vec{D} \times \vec{E} - \vec{E} \times \vec{D} \Big) + \cdots \Big\} \psi$$
$$+ \text{positron terms}$$
$$+ \text{four–fermion contact terms}$$
$$+ \text{photon terms}$$

with

$$D_t = \frac{\partial}{\partial t} + iqA^0, \quad \vec{D} = \vec{\nabla} - iq\vec{A}, \quad \vec{E} = -\vec{\nabla} A^0 - \frac{\partial \vec{A}}{\partial t}, \quad \vec{B} = \vec{\nabla} \times \vec{A}$$

The electron charge and mass are q and m

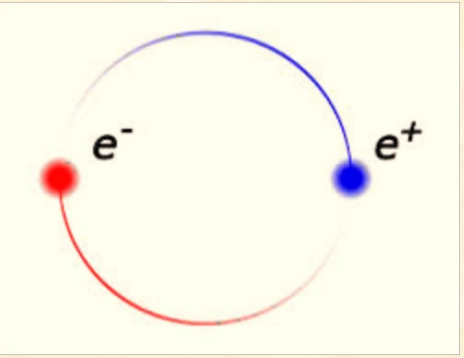

Lagrangian of NRQED

$$\mathcal{L} = \psi^\dagger \Big\{ iD_t + \frac{\vec{D}^{\,2}}{2m} + \frac{\vec{D}^{\,4}}{8m^3} + c_F \frac{q}{2m} \vec{\sigma} \cdot \vec{B} + c_D \frac{q}{2m^2} [\vec{\nabla} \cdot \vec{E}]$$
$$+ c_S \frac{iq}{8m^2} \vec{\sigma} \cdot \Big(\vec{D} \times \vec{E} - \vec{E} \times \vec{D} \Big) + \cdots \Big\} \psi$$
$$+ \text{positron terms}$$
$$+ \text{four–fermion contact terms}$$
$$+ \text{photon terms}$$

Compare with the usual QED:

$$\mathcal{L} = \bar{\psi} \left(i\gamma^\mu D_\mu - m \right) \psi + \text{photon terms}$$

with

$$D_t = \frac{\partial}{\partial t} + iqA^0, \quad \vec{D} = \vec{\nabla} - iq\vec{A}, \quad \vec{E} = -\vec{\nabla} A^0 - \frac{\partial \vec{A}}{\partial t}, \quad \vec{B} = \vec{\nabla} \times \vec{A}$$

The electron charge and mass are q and m

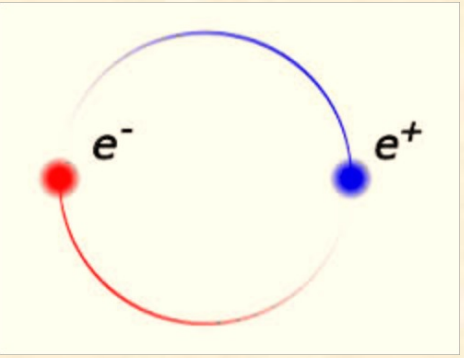

NRQED Feynman Rules

Propagators:

Coulomb photon

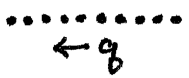

$$\frac{i}{\vec{q}^{\,2}}$$

Transverse photon

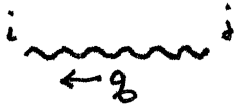

$$\frac{i\delta^T_{ij}(\vec{q})}{q^2+i\epsilon} \quad \text{where} \quad \delta^T_{ij}(\vec{q}) = \delta_{ij} - \hat{q}_i\hat{q}_j$$

Fermion
(electron or positron)

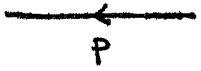

$$\frac{i}{p_0 - \frac{\vec{p}^{\,2}}{2m} + i\epsilon}$$

Interaction vertices:

Relativistic kinetic energy

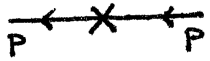

$$\frac{i}{8m^3}\vec{p}^{\,4}$$

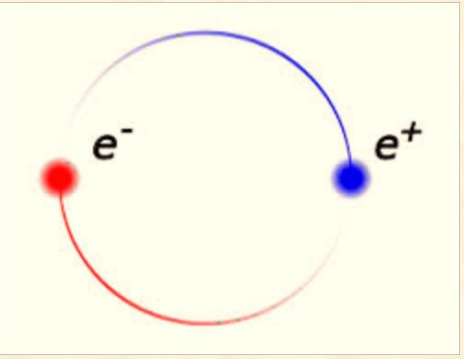

NRQED Feynman Rules

Interaction vertices:

Coulomb 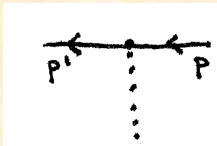

$-iq$

Convection 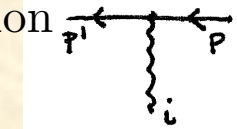

$\frac{iq}{2m}(p'+p)_i$

Fermi 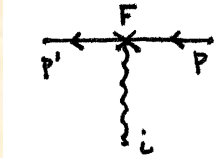

$c_F \frac{q}{2m}\left((\vec{p}\,' - \vec{p}\,) \times \vec{\sigma}\,\right)_i$

Contact 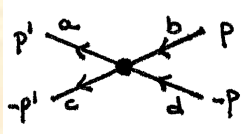

$\frac{d_2}{m^2}\delta_{ab}\delta_{cd} + \frac{d_v}{m^2}\vec{\sigma}_{ab}\cdot\vec{\sigma}_{cd}$

Spin − orbit 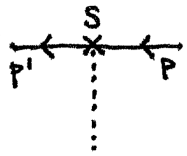

$c_S \frac{q}{4m^2}\left((\vec{p}\,' \times \vec{p}\,)\cdot\vec{\sigma}\right)_i$

Darwin 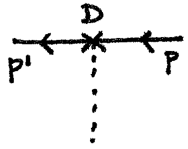

$c_D \frac{iq}{8m^2}(\vec{p}\,' - \vec{p}\,)^2$

Seagull 

$\frac{-iq^2}{2m}\delta_{ij}$

$+\cdots$

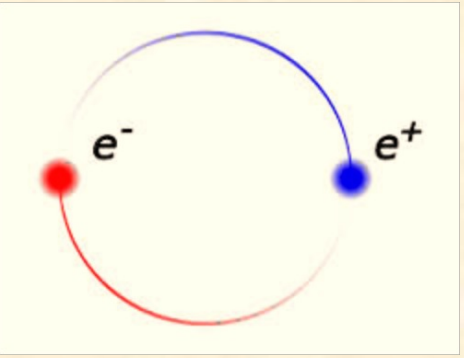

Lagrangian of NRQED

$$\mathcal{L} = \psi^\dagger \Big\{ iD_t + \frac{\vec{D}^{\,2}}{2m} + \frac{\vec{D}^{\,4}}{8m^3} + c_F \frac{q}{2m} \vec{\sigma} \cdot \vec{B} + c_D \frac{q}{2m^2} [\vec{\nabla} \cdot \vec{E}]$$
$$+ c_S \frac{iq}{8m^2} \vec{\sigma} \cdot \Big(\vec{D} \times \vec{E} - \vec{E} \times \vec{D} \Big) + \cdots \Big\} \psi$$
$$+ \text{positron terms}$$
$$+ \text{four–fermion contact terms}$$
$$+ \text{photon terms}$$

The matching coefficients have the values

$$c_F = 1 + \frac{\alpha}{2\pi} + \cdots$$

$$c_D = 1 + \frac{8\alpha}{3\pi} \left\{ \frac{-1}{2\epsilon} + \ln \frac{m}{\mu} \right\} + \cdots$$

$$c_S = 1 + \frac{\alpha}{\pi} + \cdots$$

(using dimensional regularization in $d = 4 - 2\epsilon$ dimensions)

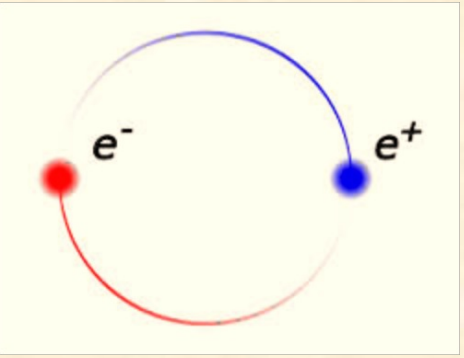

Contact Term

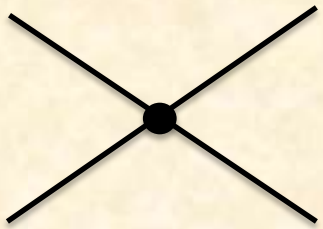

The contact interaction includes the effects of all annihilation contributions:

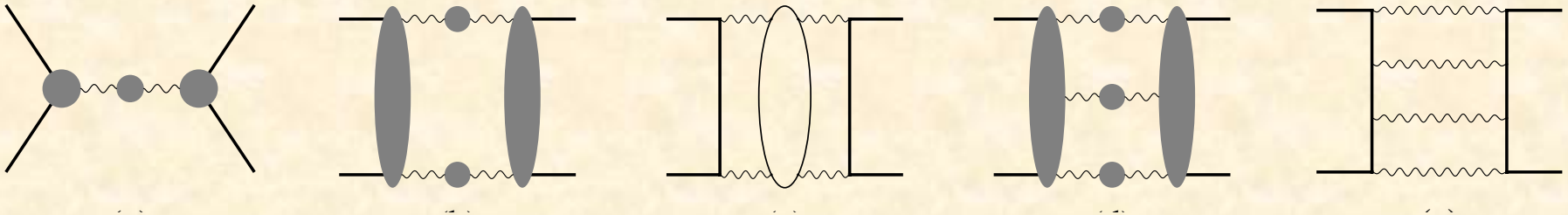

plus the relativistic (short distance) parts of the exchange contributions:

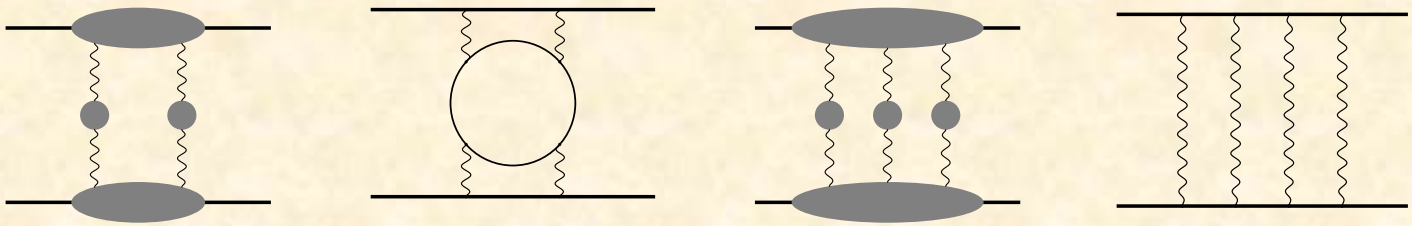

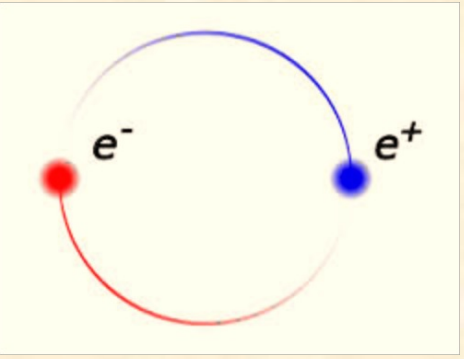

NRQED Kernels for the Fine Structure

The kernels that contribute to energies at order $m\alpha^4$ are shown below:

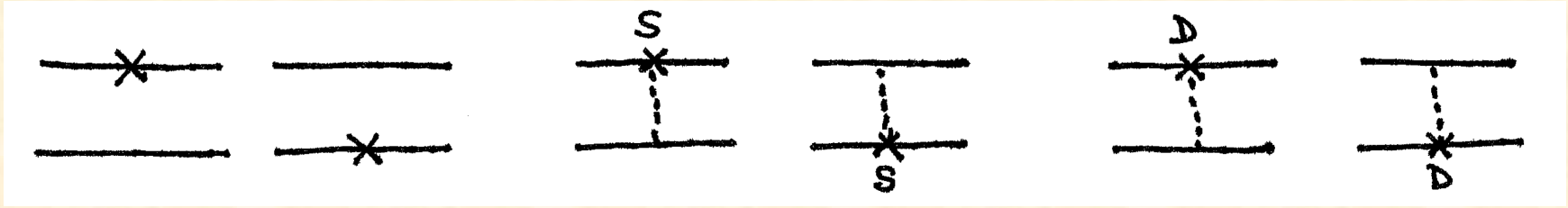

Relativistic kinetic energy

Spin – orbit

Darwin

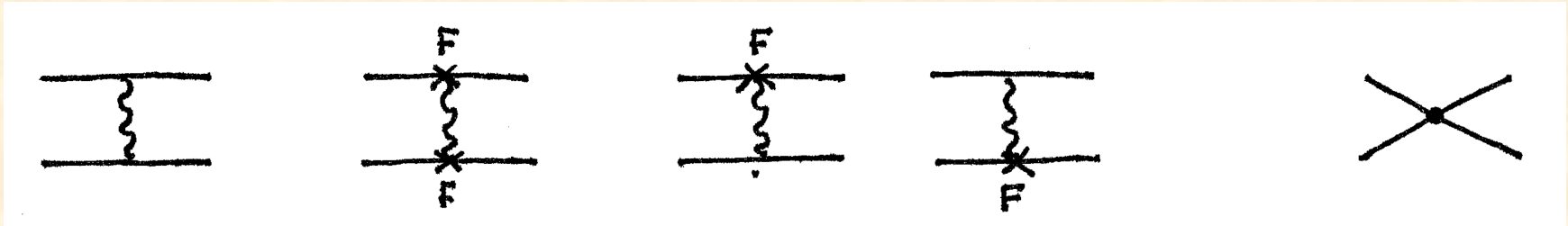

Transverse

Fermi spin-spin

Fermi spin-orbit

Contact

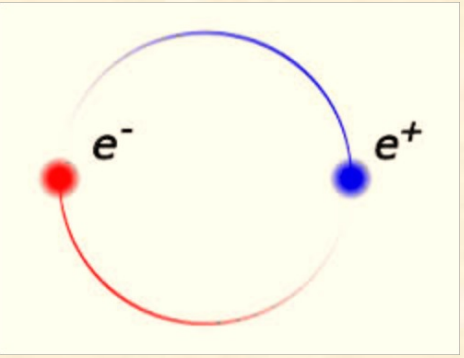

Order α^7 Energy Corrections

Contributions to energies at order $m\alpha^7$ can be organized by the number of photon involved (at least for hard, i.e. high energy photons). Terms with four hard photons contribute at order $m\alpha^7$: α^4 from the explicit photons and α^3 from the wave function at spatial contact. The relevant graphs are shown below. (Shaded blobs indicate fully corrected vertex parts, fully corrected propagators, etc.)

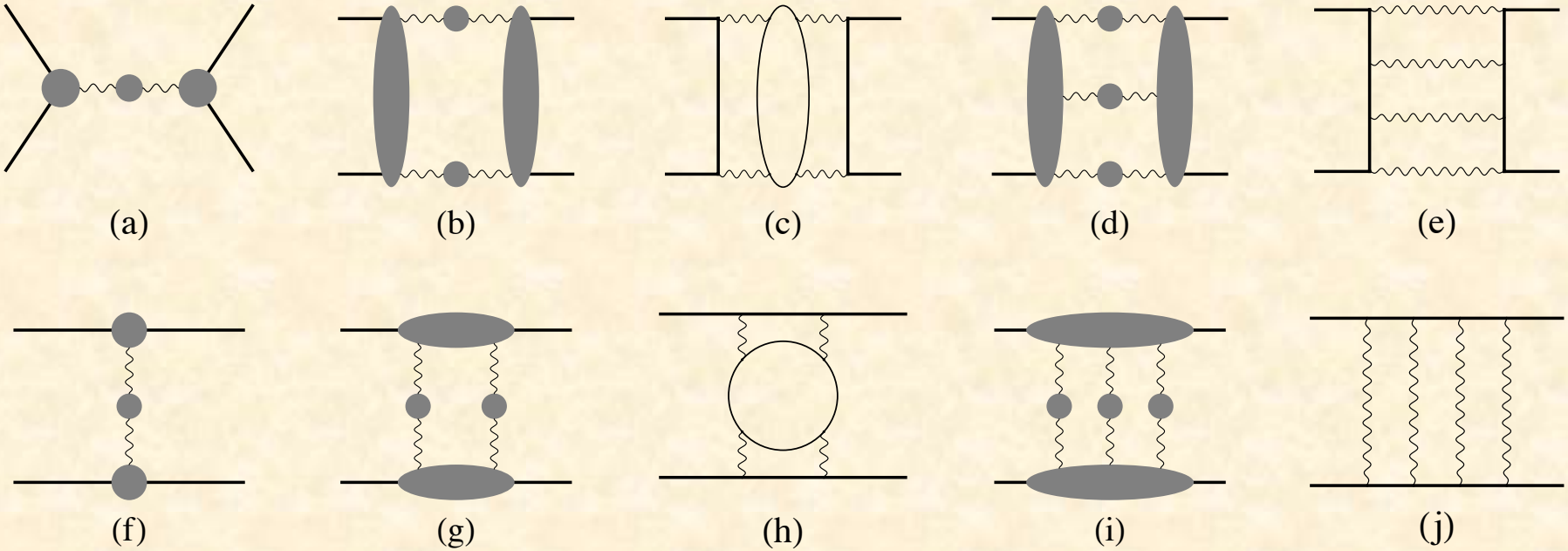

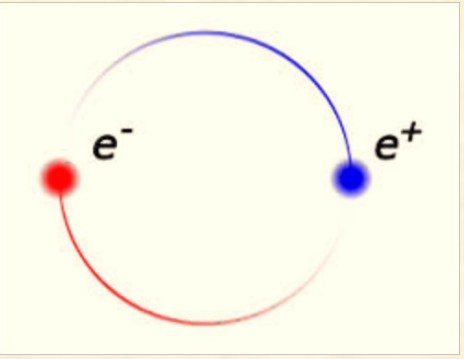

Order α^7 Energy Corrections

Marcu (2011) evaluated the contribution of ultrasoft photon exchange to the hyperfine splitting using the effective non-relativistic field theory pNRQED ("potential"–NRQED). Her anomalously large result was

$$\Delta E = 108.6 \frac{m\alpha^7}{\pi^3} = 0.477 MHz$$

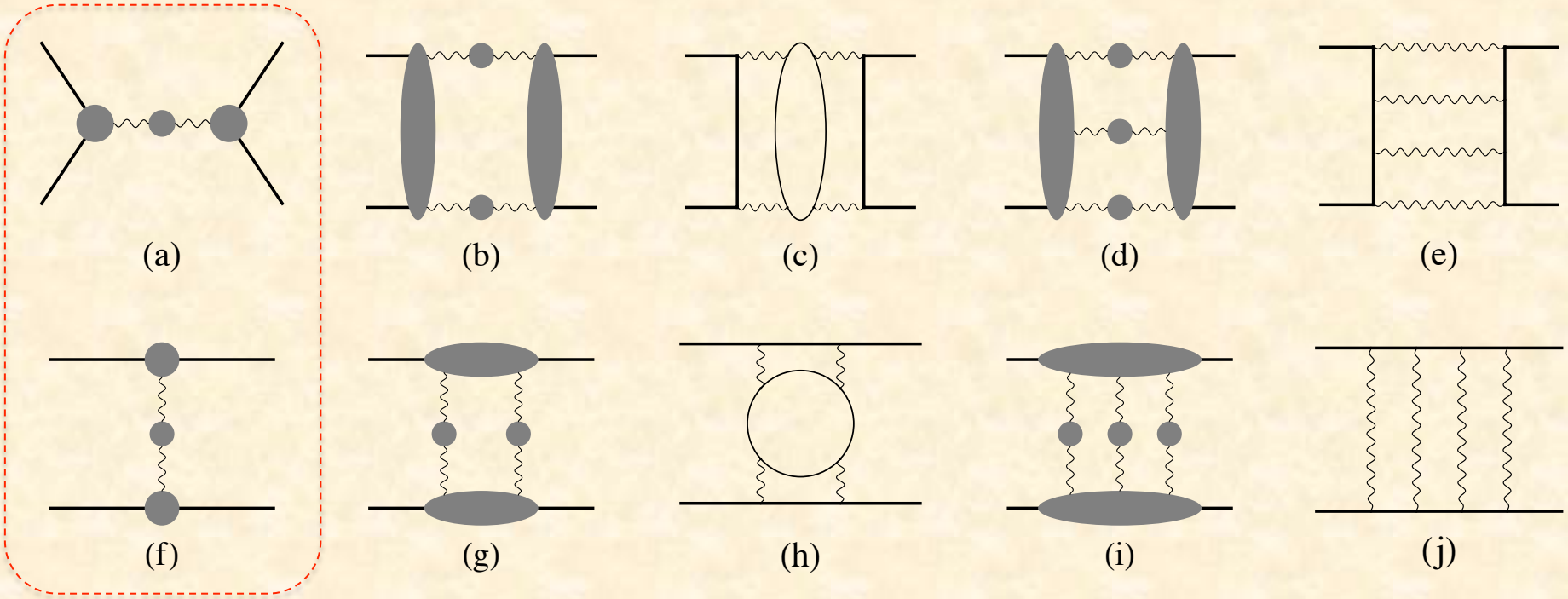

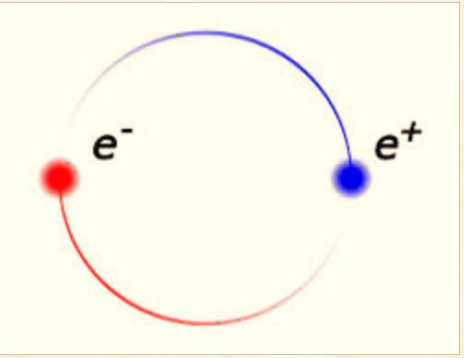

Order α^7 Energy Corrections

Adkins and Fell (2014) evaluated the contributions to the hyperfine splitting from light-by-light scattering in the exchange channel with the result

$$\Delta E = -0.2354 \frac{m\alpha^7}{\pi^3} = -1.033 kHz$$

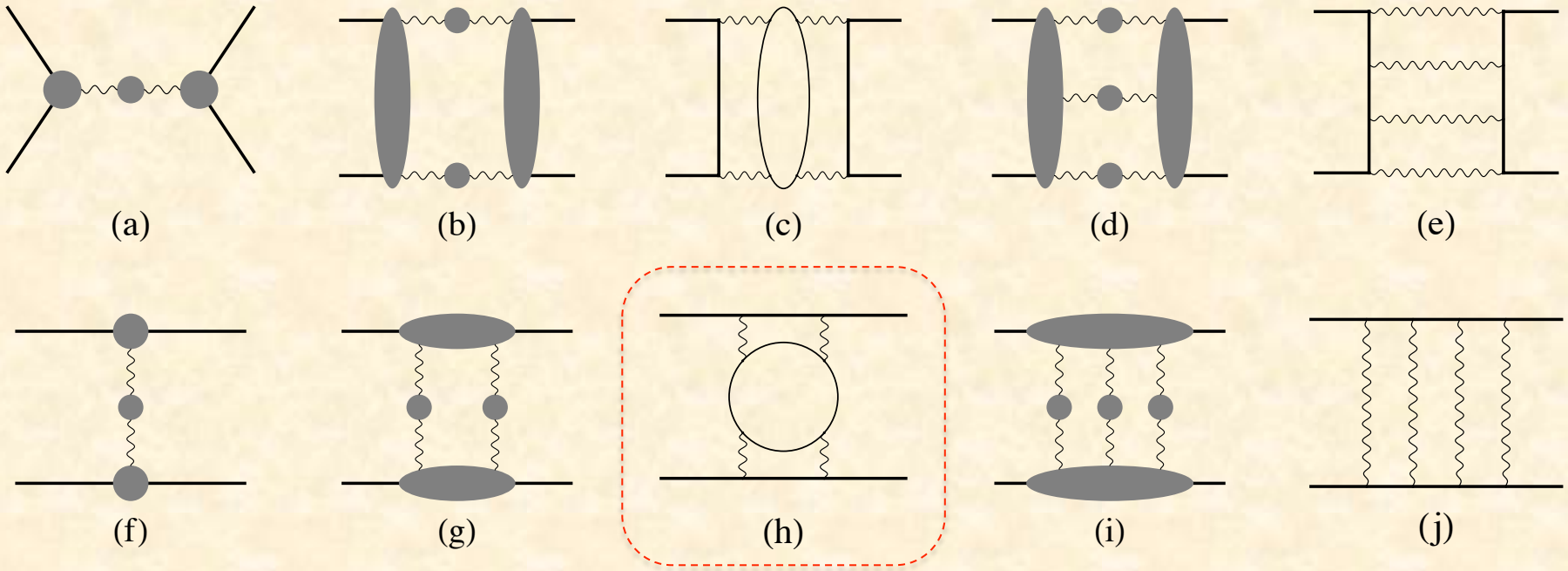

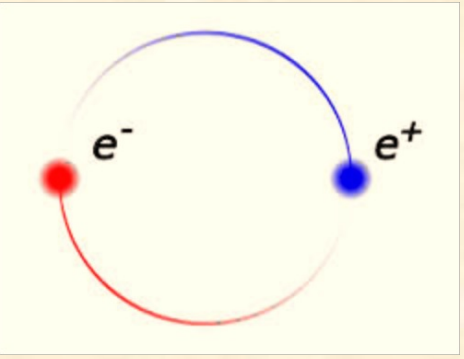

Order α^7 Energy Corrections

Eides and Shelyuto (2014) evaluated the contributions to the hyperfine splitting from two-photon-exchange graphs involving "hard" photons exclusively. Their result is

$$\Delta E = -1.2917(1)\frac{m\alpha^7}{\pi^3} = -5.672kHz$$

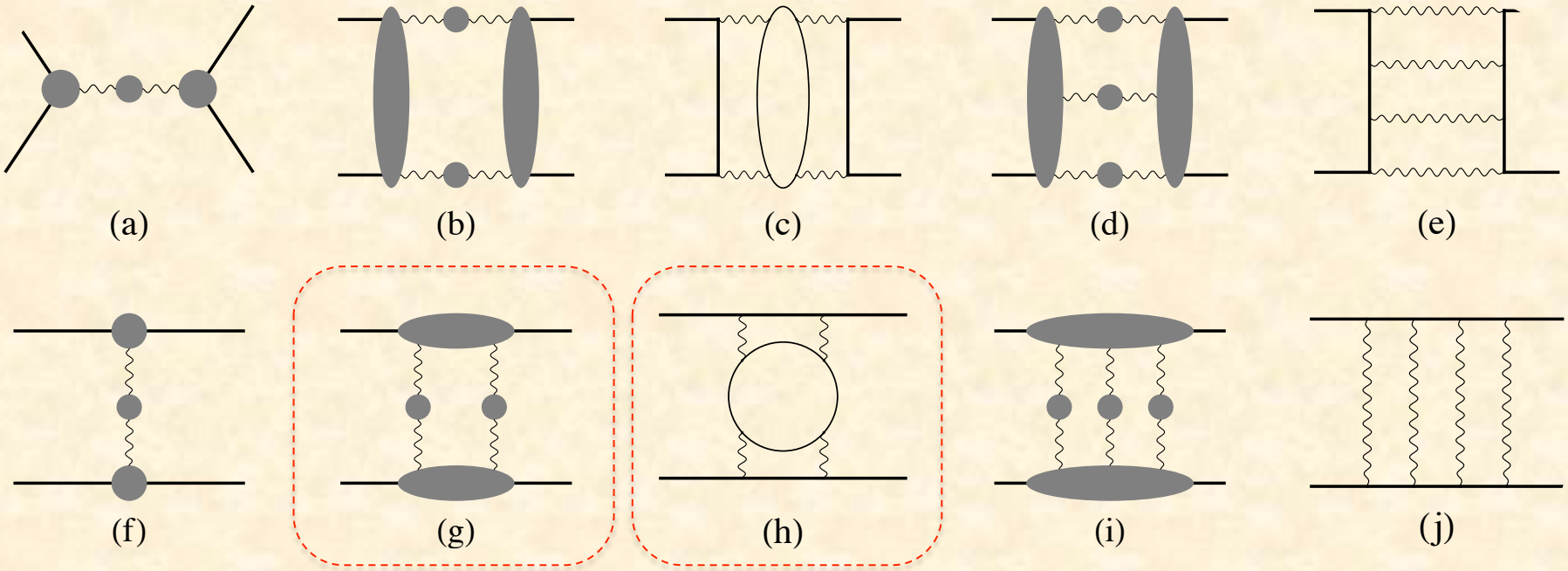

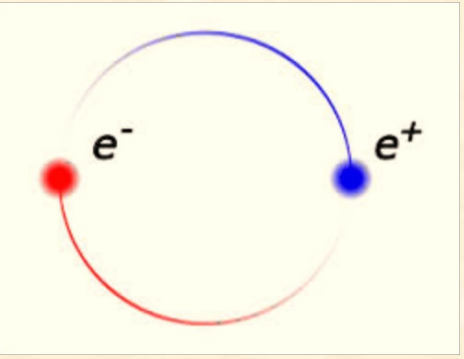

Order α^7 Energy Corrections

Baker, Marquard, Penin, Piclum, and Steinhauser (2014) obtained the complete result for the one-photon-annihilation contribution—including the ultrasoft part:

$$\Delta E = 49.5(3)\,\frac{m\alpha^7}{\pi^3} = 0.2174(13)MHz$$

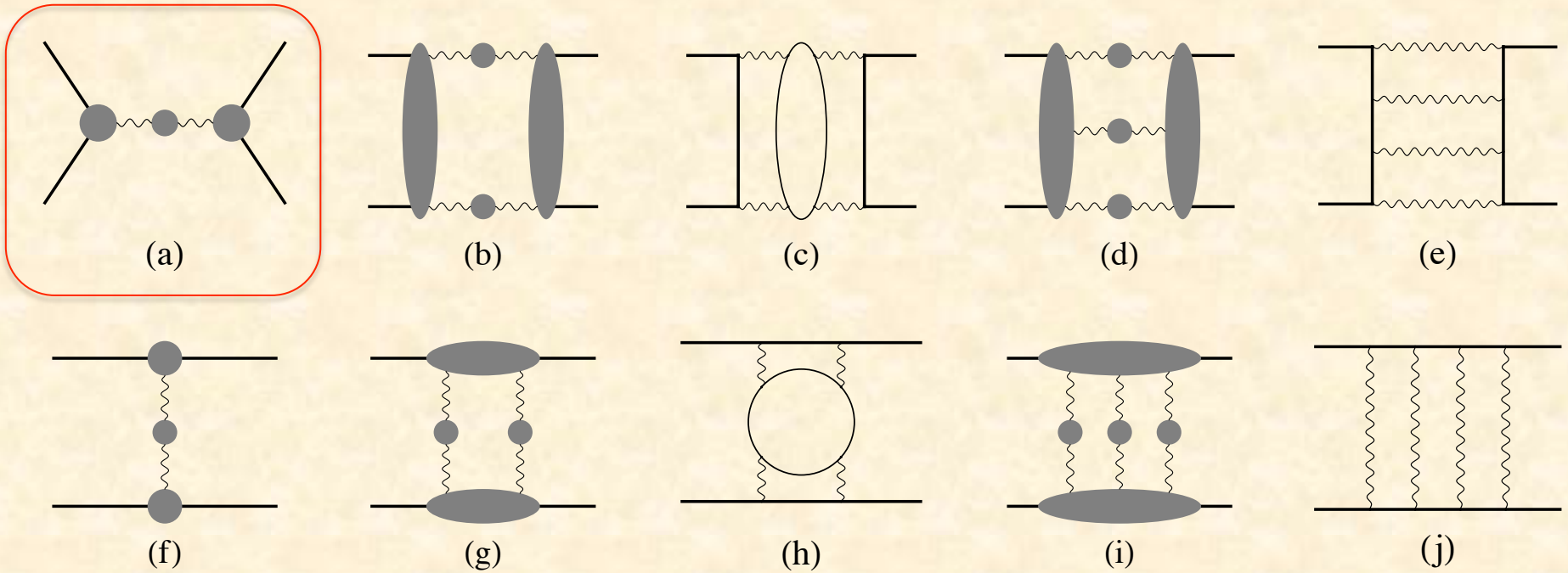

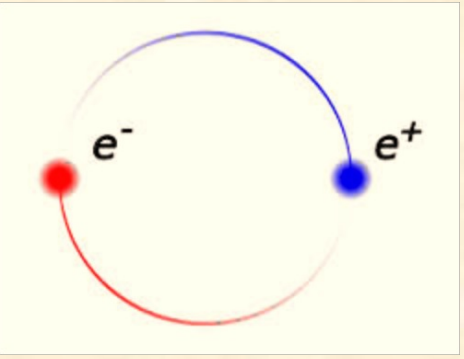

Order α^7 Energy Corrections

Parts of the two-photon-annihilation contribution [graphs (b) and (c)] and the complete three-photon-annihilation contribution [graph(d)] have been done:

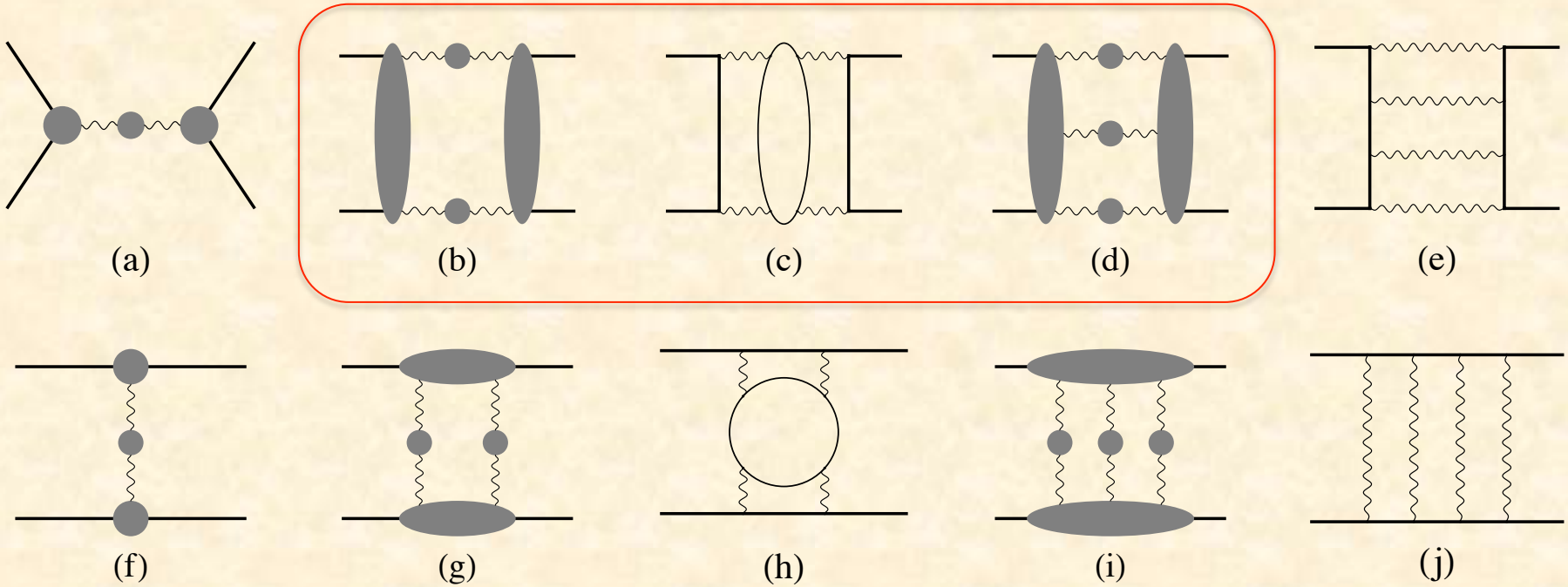

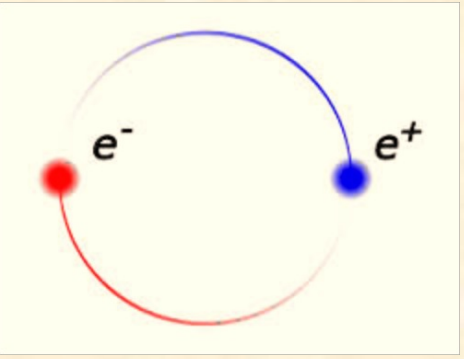

Two-photon-annihilation contributions to positronium energy levels

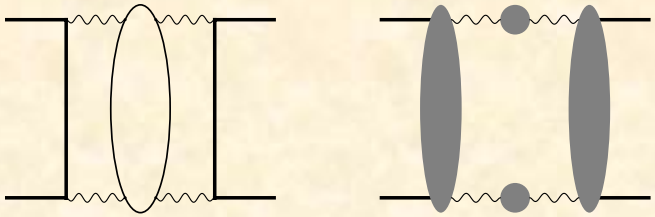

The generic two-photon-annihilation graphs are shown above. In expanded form, they are shown at right as the

(a) light-by-light
(b) vacuum polarization
(c) product (of two one-loop terms)
(d) two-loop terms

So far, parts (a), (b), and (c) are complete.

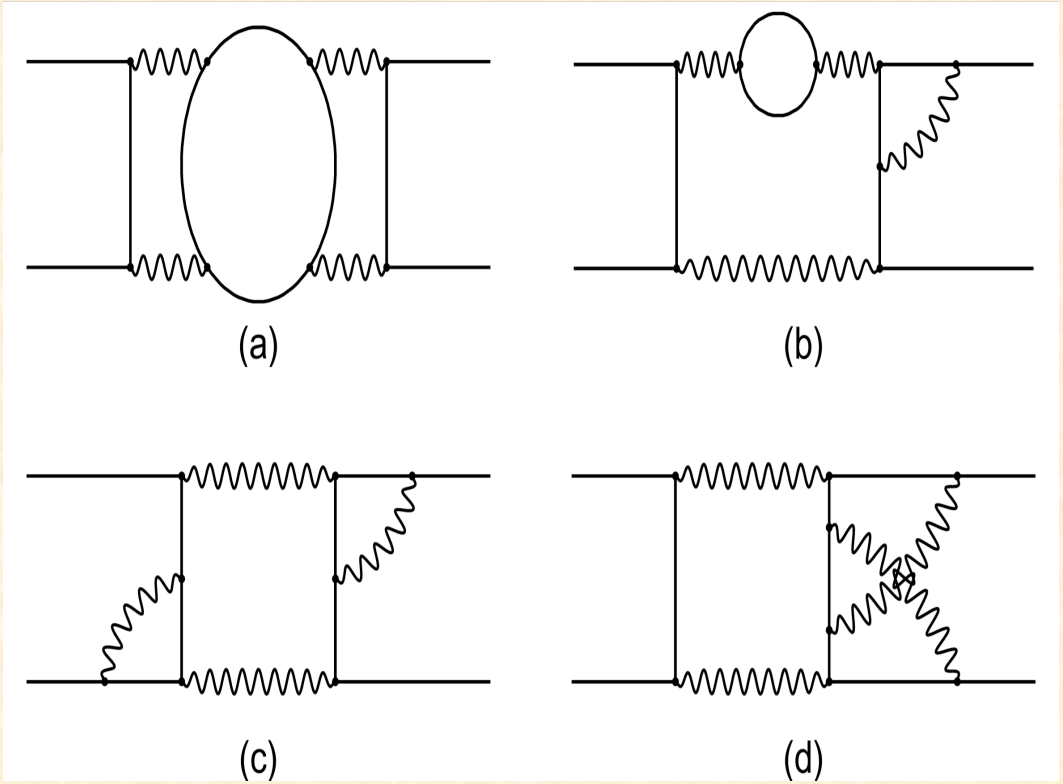

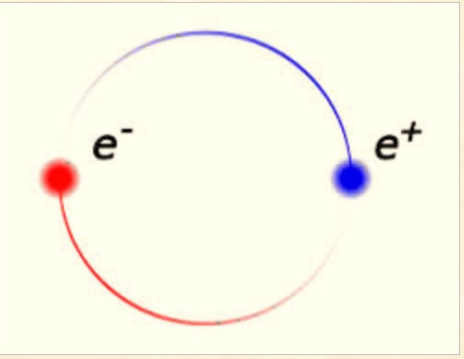

Two-photon-annihilation contributions to positronium energy levels

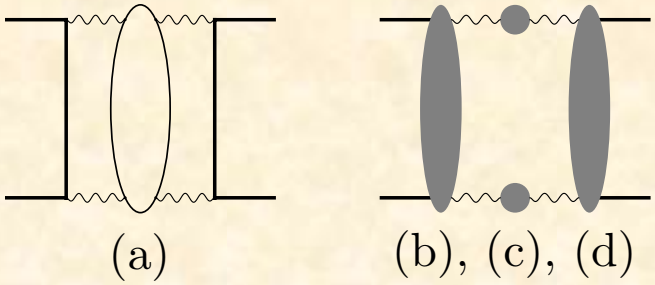

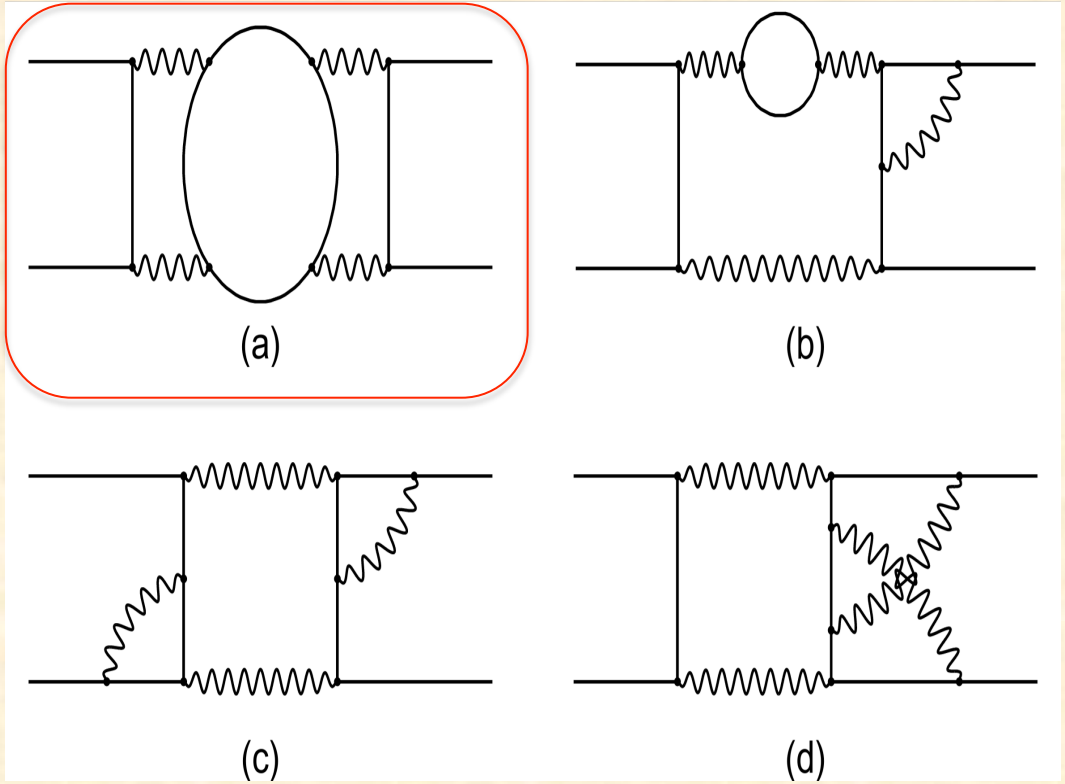

The generic two-photon-annihilation graphs are shown above. In expanded form, they are shown at right as the

(a) light-by-light
(b) vacuum polarization
(c) product (of two one-loop terms)
(d) two-loop terms

Result for (a):

$$\Delta E = \{1.583 - 1.016\,i\}\,\frac{m\alpha^7}{\pi^3} = -6.95 kHz + \cdots$$

(Adkins, Fell, Parsons, Salinger, and Wang, 2014)

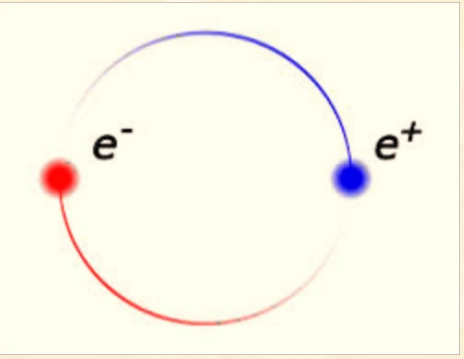

Two-photon-annihilation contributions to positronium energy levels

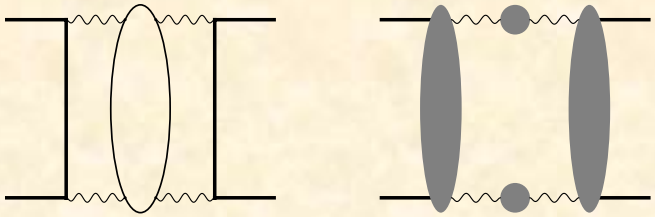

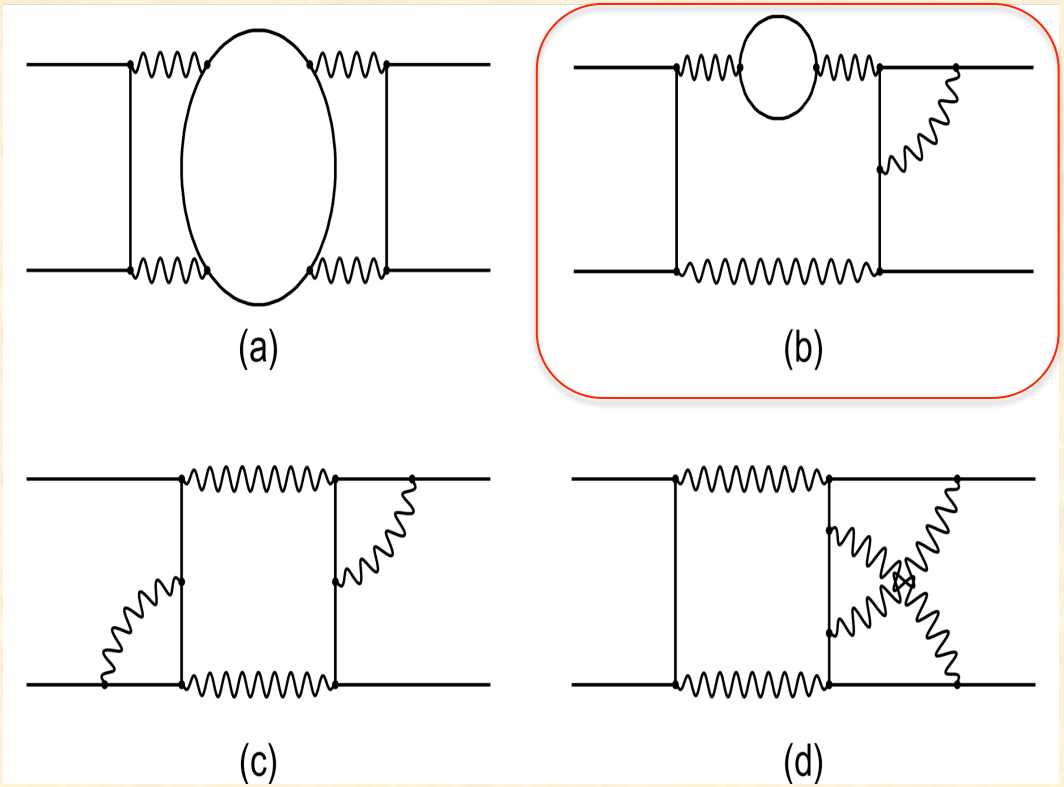

The generic two-photon-annihilation graphs are shown above. In expanded form, they are shown at right as the

(a) light-by-light
(b) vacuum polarization
(c) product (of two one-loop terms)
(d) two-loop terms

Result for (b): $$\Delta E = -0.153095(3)\frac{m\alpha^7}{\pi^3} = 0.67kHz + \cdots$$

(Adkins, Parsons, Salinger, and Wang, 2015)

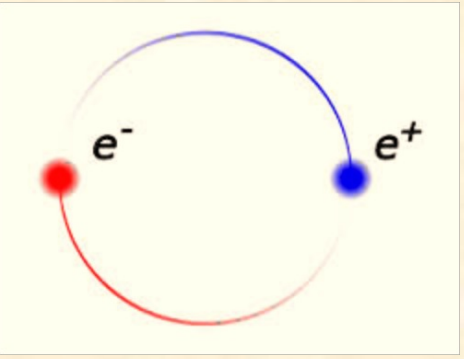

Two-photon-annihilation contributions to positronium energy levels

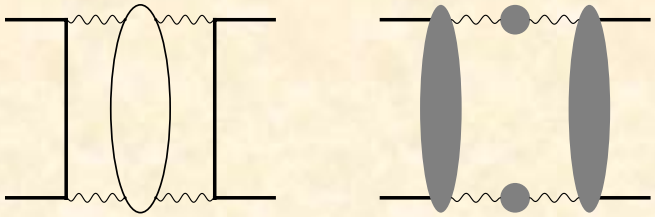

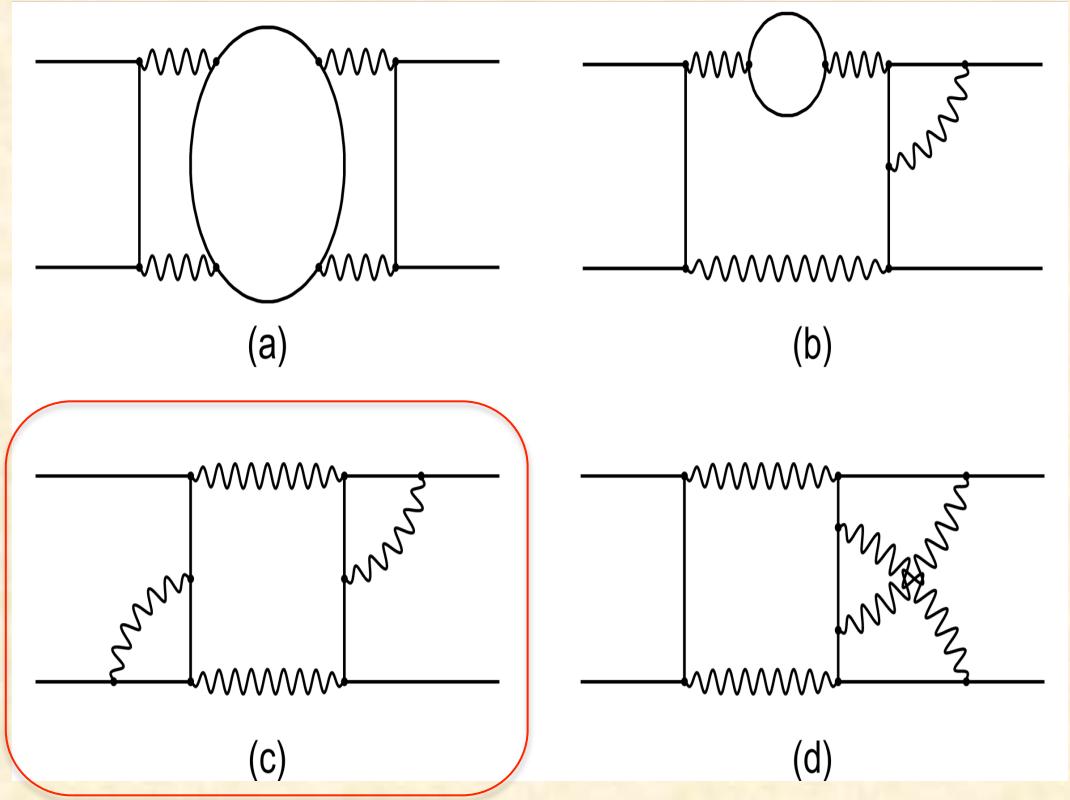

The generic two-photon-annihilation graphs are shown above. In expanded form, they are shown at right as the

(a) light-by-light
(b) vacuum polarization
(c) product (of two one-loop terms)
(d) two-loop terms

Result for (c):

$$\Delta E = \{-0.5620 - 1.259\,i\}\,\frac{m\alpha^7}{\pi^3} = -2.47 kHz + \cdots$$

(Adkins, Tran, and Wang, 2016)

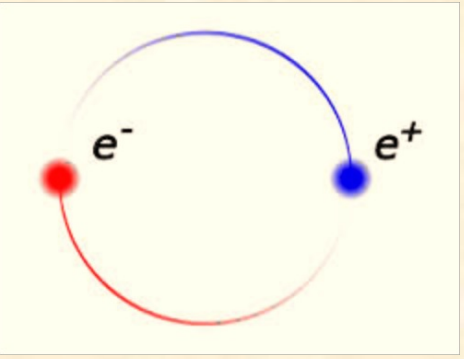

Two-photon-annihilation contributions to positronium energy levels

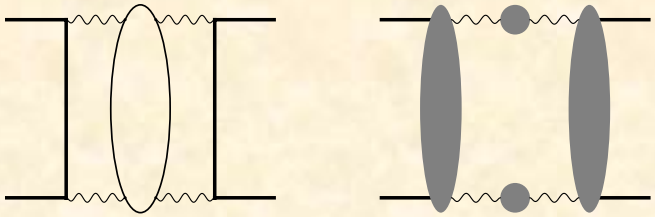

The generic two-photon-annihilation graphs are shown above. In expanded form, they are shown at right as the

(a) light-by-light
(b) vacuum polarization
(c) product (of two one-loop terms)
(d) two-loop terms

The result for (d) is not yet complete.

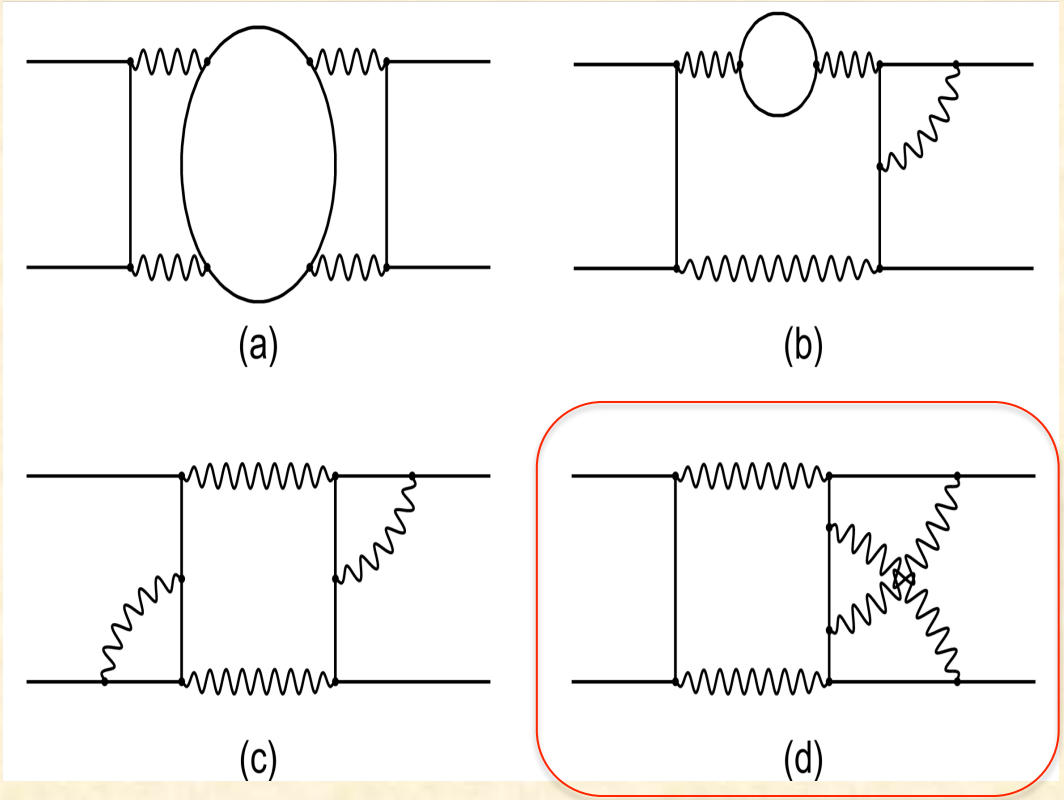

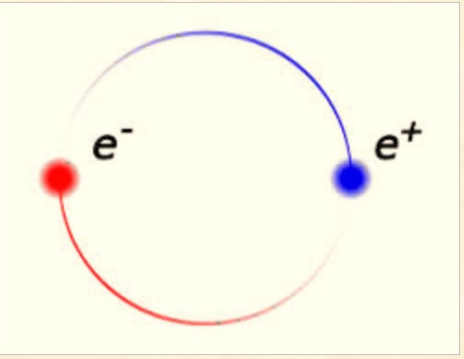

Three-photon-annihilation contributions to positronium energy levels

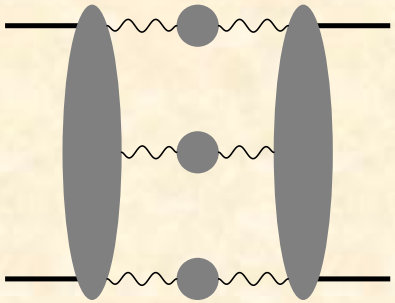

The generic three-photon-annihilation graph shown above expands into the graphs shown to the right when evaluated to order $m\alpha^7$. The graphs shown are only representative of the actual contributions.

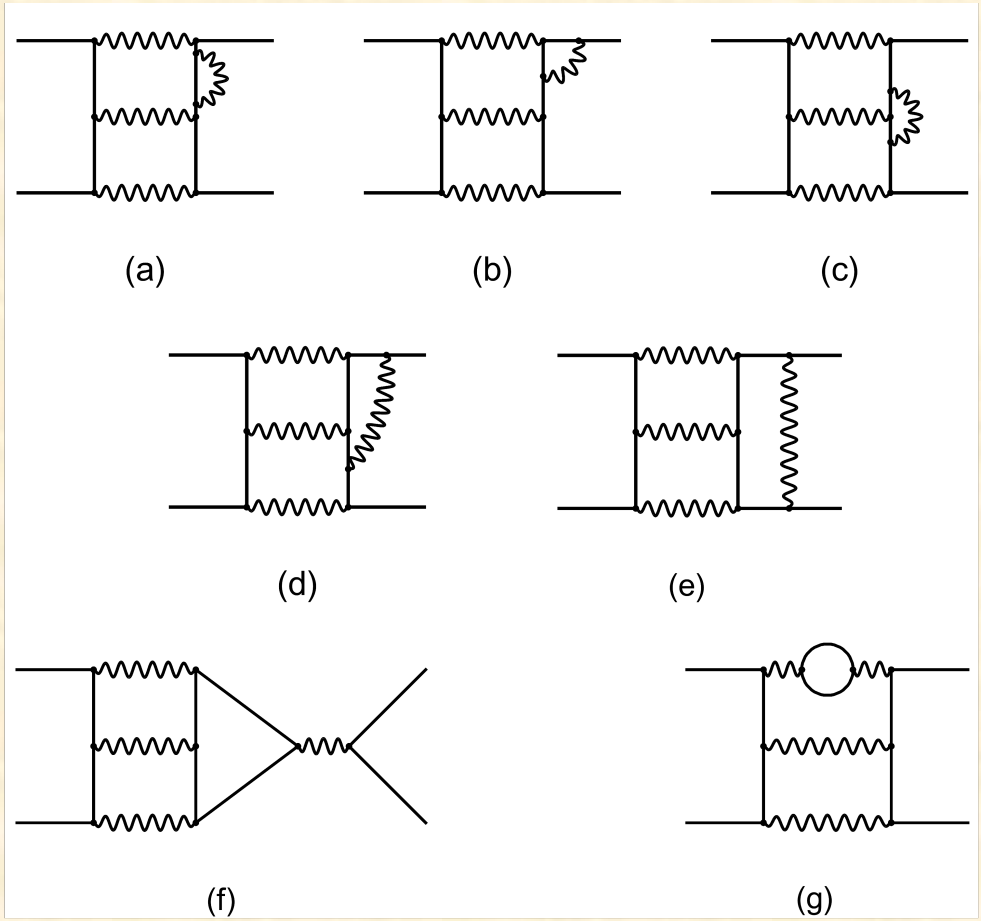

The total three-photon-annihilation contribution is:

$$\Delta E = \{2.622 + 3.123\,i\}\,\frac{m\alpha^7}{\pi^3} = 11.5kHz + \cdots$$

(Adkins, Fell, Kim, and Parsons, 2016)

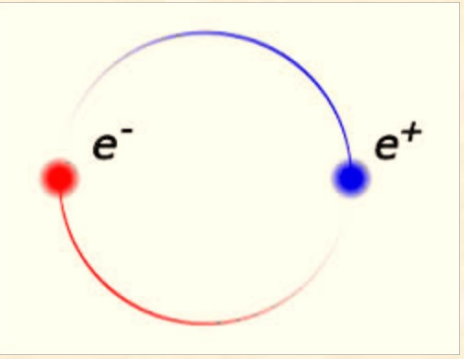

Order α^7 Energy Corrections

Summary of completed contributions (solid line boxes) and partially completed contributions (dashed line boxes):

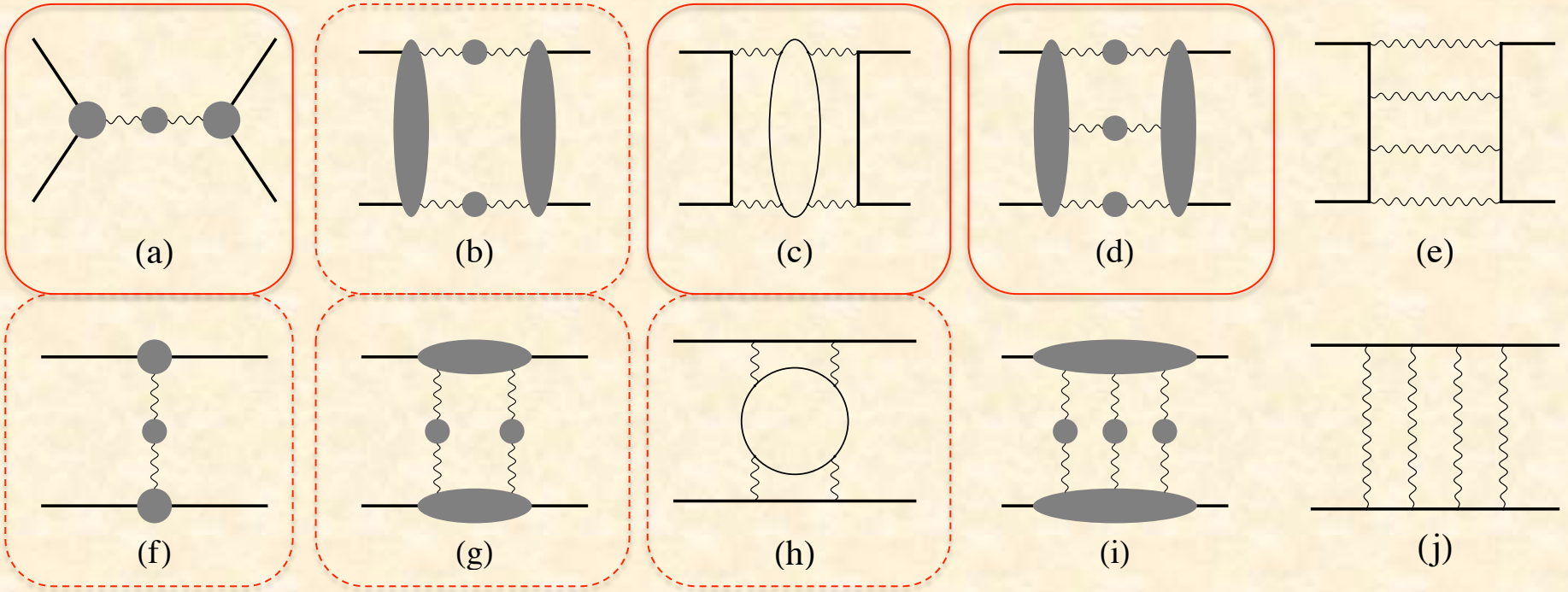

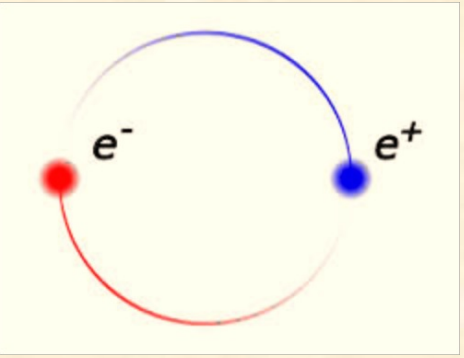

Order α^7 Contributions to the Hyperfine Splitting

Summary

Ultrasoft: annihilation channel	204.4 kHz
Additional one-photon-annihilation contributions	12.8(1.3) kHz
Two-photon-annihilation contributions	3.1 kHz
Light-by-light: annihilation channel	-6.9 kHz
Three-photon-annihilation contributions	11.5 kHz
Ultrasoft: exchange channel	272.5 kHz
Anomalous moment in one-photon-exchange	3.0 kHz
Light-by-light: exchange channel	-1.0 kHz
Other two-photon-exchange contributions	-4.7 kHz
Total (very incomplete)	494.7 kHz

Thank you!

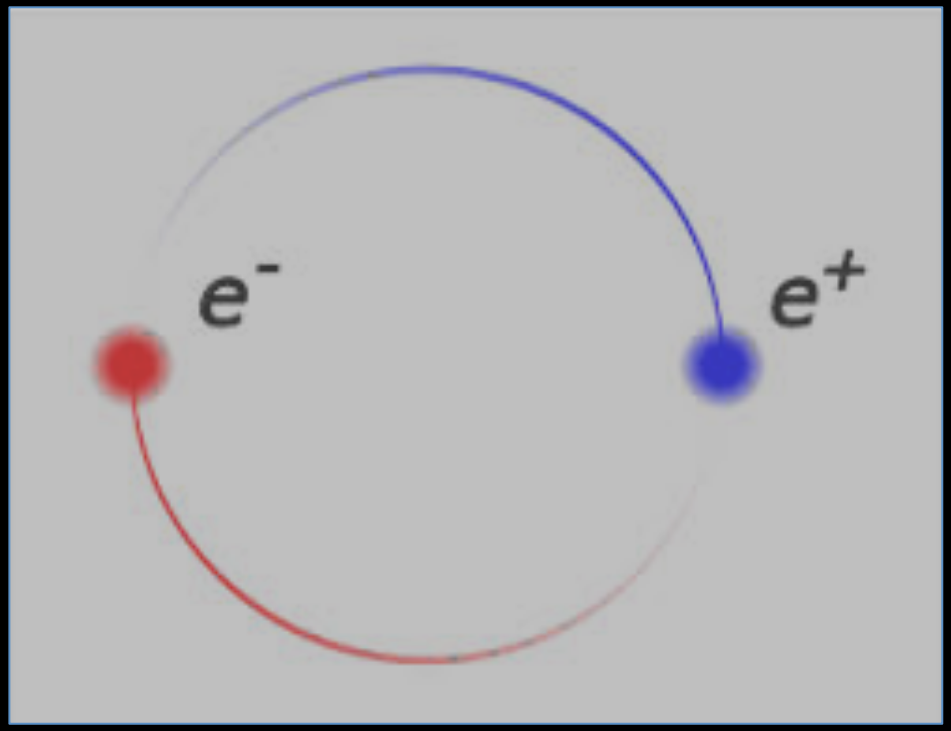

Greg Adkins
Franklin & Marshall College

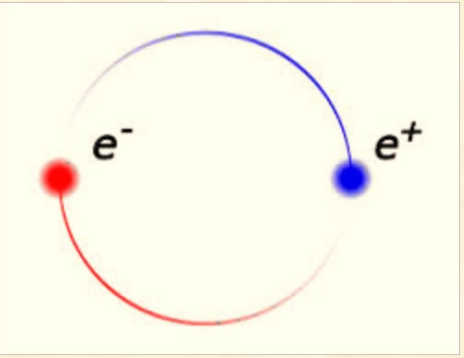

NRQED Feynman Rules

Dressing the fermion propagator:

The bare fermion propagator $\dfrac{i}{p_0 - \frac{\vec{p}^{\,2}}{2m} + i\epsilon}$ corrected by multiple insertions of the relativistic kinetic energy vertex $\dfrac{i}{8m^3}\vec{p}^{\,4}$ gives a series that can be summed as a geometric series:

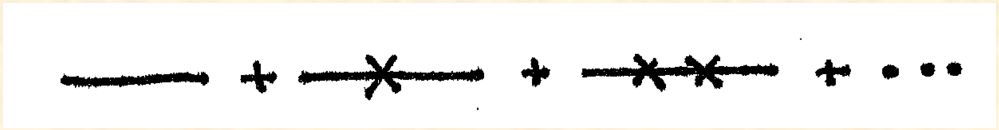

$$= \frac{i}{p_0 - \frac{\vec{p}^{\,2}}{2m} + \frac{\vec{p}^{\,4}}{8m^3} + i\epsilon}$$

building up the full propagator with the correct relativistic kinetic energy:

$$\sqrt{m^2 + \vec{p}^{\,2}} - m = \frac{\vec{p}^{\,2}}{2m} - \frac{\vec{p}^{\,4}}{8m^3} + \cdots$$